J. Fluid Mech. (1986), *vol.* 165, *pp.* 475–501
Printed in Great Britain

Velocity fluctuations near an interface between a turbulent region and a stably stratified layer

By D. J. CARRUTHERS† AND J. C. R. HUNT
Department of Applied Mathematics and Theoretical Physics, University of Cambridge, Silver Street, Cambridge CB3 9EW

(Received 13 March 1984 and in revised form 17 September 1985)

Velocity fluctuations are calculated near an interface between a turbulent region and a stably stratified layer, and in the absence of mean shear. Based on the observation that the energy dissipation rate is finite in the turbulent region, a linear theory is constructed to match the given Eulerian (*not* Lagrangian) spectra of the turbulence in the turbulent region to the wave motion in the stable layer.

The theory shows that eddies with frequency of the same order as the buoyancy frequency N of the stratified layer are least affected by the stratification. The mean square vertical velocity $\overline{w^2} \to 0$ when $N \to \infty$, while $\overline{w^2}$ is greatest at the interface when $NL_H/u_H \approx 2$; u_H and L_H are respectively the velocity scale and longitudinal integral scale in the interior of the turbulent layer. In the stratified layer, since waves with frequency $\omega > N$ decay rapidly with distance z from the interface, the high-frequency parts of the spectra fall-off sharply, a striking feature of the atmospheric measurements of Caughey & Palmer (1979). In this inviscid model waves with frequency $\omega < N$ propagate in the stratified region without decay. The vertical integral scale $L_x^{(w)}$ is found to vary significantly with N, reaching a maximum at the interface when $NL_H/u_H \approx 1$. The wave energy flux (F_w) is a maximum when $NL_H/u_H \approx 6$, a value frequently observed in the atmosphere.

In the limit of large stratification ($N \to \infty$), the theory shows that the effect of the stable layer on the turbulent region is the same as that of a rigid surface moving with the flow at the same mean velocity (i.e. the solution of Hunt & Graham 1978). Then $F_w \to 0$ and, at the interface, $L_x^{(w)} \to 0$. In the limit of small stratification ($N \to 0$) the vertical motion in the turbulent region decreases in intensity near the interface and irrotational motions are induced in the slightly stable layer (i.e. the same result as Phillips 1955).

1. Introduction

There are many natural flows where regions of turbulent motion adjoin regions of stably stratified fluid in which there is no local production of turbulence. These include the upper part of the atmospheric convective boundary layer which is capped by an inversion, the oceanic mixed layers, at the base of which is the thermocline, and stellar convection zones bounded by stably stratified regions. The interaction between the turbulent region and stratified layers needs to be better understood because it affects and often controls the movement of the interface dz_i/dt and fluxes of momentum F and scalar quantities F_s across the interface. For instance, in

† Present address: Department of Atmospheric Physics, Clarendon Laboratory, Parks Road, Oxford.

large-scale numerical-model studies of the atmosphere, these quantities are estimated from physical arguments and experimental data in terms of various local physical quantities.

It is convenient to subdivide the general class of turbulent flows confined by stratification into three main types of flow, all of which occur frequently. (We assume there is no potential temperature gradient in the turbulent layer.)

(i) The stable layer has a uniform density or temperature gradient as in the experiments of Willis & Deardorff (1974), and the atmospheric measurements of Caughey & Palmer (1979). There is no mean shear.

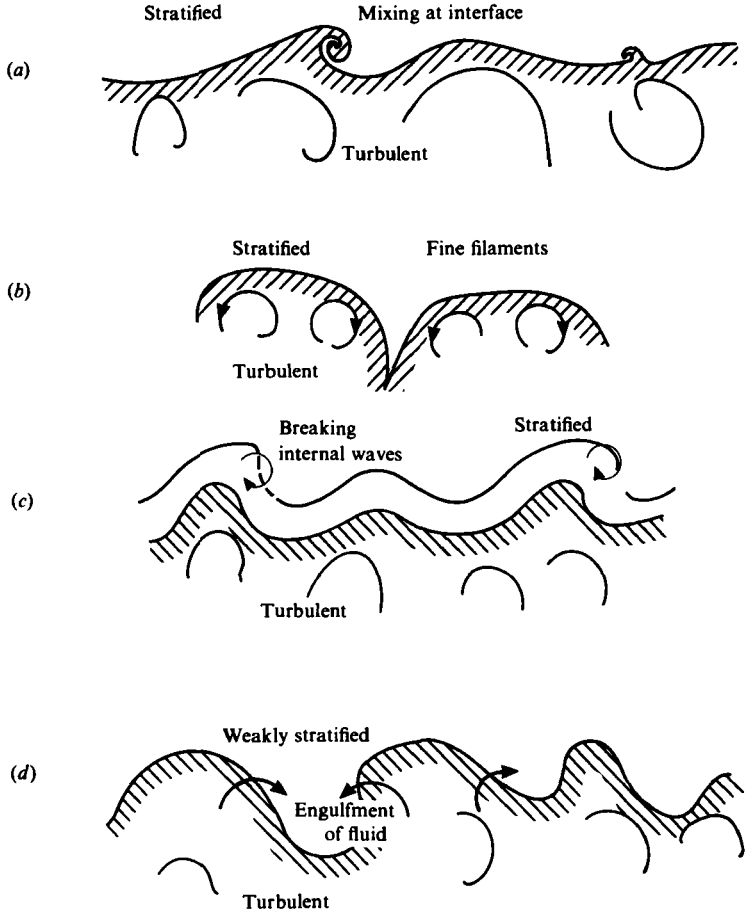

FIGURE 1. Mechanisms of entrainment. (*a*) Mixing due to fluctuating velocities at an interface. (*b*) Fine filaments entrained by energetic eddies. (*c*) Waves breaking in stratified fluid. (*d*) Engulfment of fluid of weak stratification.

(ii) There is an intensely stratified layer marking the edge of the turbulent layer with fluid of lower stratification (which may be neutral) beyond, as for example in the atmospheric measurements of Caughey, Crease & Roach (1982). There is no mean shear.

(iii) Either of the above cases with mean shear. This shear is usually most intense when it is associated with a narrow stably stratified layer (Brost, Wyngaard & Lenshow 1982).

A large number of laboratory experiments have been performed to measure the rate of growth of the thickness z_1 of the turbulent layer and the fluxes for each of the above cases. Both these kinds of measurements are often expressed as 'entrainment velocities' E, where $E = \mathrm{d}z_1/\mathrm{d}t$ or $E = F_s/\Delta S$, where ΔS is the change in the value across the layer. Numerous attempts have been made to relate these entrainment velocities to the bulk properties of the flow (e.g. Kato & Phillips 1969; Kantha, Phillips & Azad 1978; Price 1979; Turner 1973; Willis & Deardorff 1974; Piat & Hopfinger 1981).

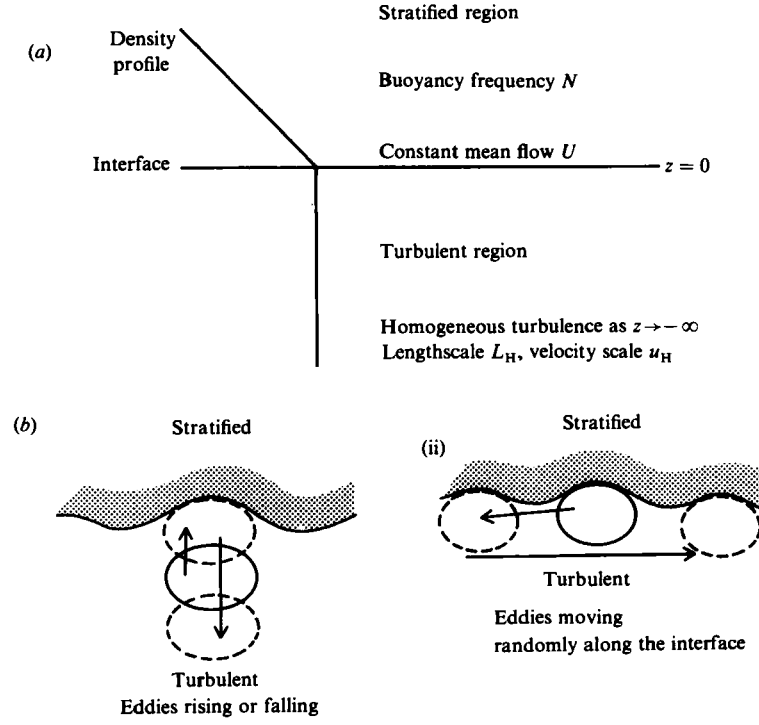

FIGURE 2. (*a*) Pictorial representation of the flow field described by the theory. (*b*) Physical picture of the use of the different frequency spectra; the eddies are shown at the times t_0, t_1, t_2 and $t_0 < t_1 < t_2$; (i) Lagrangian spectrum: eddies rising or falling. (ii) Eulerian spectrum: eddies randomly moving along the interface.

Four distinct mechanisms have been proposed for the entrainment process (figure 1) (though they have never been systematically compared).

(*a*) Turbulent eddies impinge on the interface and generate sufficiently large fluctuating-velocity gradients at the interface that the local Richardson number $g(\partial\bar{\theta}/\partial z)/\bar{\theta}(\partial u/\partial z)^2$ is small enough for Kelvin–Helmholtz billows to grow and break and induce molecular mixing.

(*b*) With strong stratification and energetic turbulence, eddies impinging onto the interface distort it sufficiently that fine filaments of the stratified fluid layer are entrained into the turbulent region, where again molecular diffusion completes the mixing process (Linden 1973). Linden hypothesized that eddies are similar to vortex rings and then, by experiment and approximate analysis, he was able to estimate entrainment rates across a density discontinuity.

(*c*) Turbulent eddies distort the interface and set up internal waves in the stratified layer whose energy and form depend on the stratification. For a uniformly stratified

layer (figure 2*a*), the waves propagate energy away from the interface but the wave amplitude at the interface may be large enough to induce mixing. If the stratified layer is strong near the interface and weak or non-existent far above it, then trapped and resonant waves of large amplitude can be induced by quite weak turbulence.

(*d*) With weak stratification the turbulent layer can also grow and entrain by the same processes as occur at the edge of a turbulent boundary layer or wake in neutral stratification; the large eddies in the turbulent layer induce large random motions in the external layer leading to the engulfment of external fluid. In the limit of zero stratification, the velocity fluctuations in the laminar layer have been shown to be irrotational and described by Phillips' (1955) theory.

In this paper we develop a linear analysis to describe the velocity fluctuations near a single interface separating a uniformly stratified layer from a turbulent layer, i.e. we investigate class (i) of the three classes of flows outlined above, in which a turbulent region is confined by stratification. A subsequent paper will describe analysis of the second class of flows. We also compare the results of the analysis with observations of velocity fluctuations. We note that linear analysis may be appropriate for such a comparison, because much of the time these fluctuations are associated with small deformations of the interface. But the linear analysis is not appropriate for calculating the nonlinear mixing processes involved in entrainment because these are often associated with large deformations of the interface. However, the theory of this and the subsequent paper may provide a method for identifying under what circumstances which of the mechanisms described above may control entrainment, since all the mechanisms are sensitive to the local fluctuating velocity field near the surface.

The linear theory developed here is a modification of the model of Hunt & Graham (1978) for turbulence in a zero-mean-shear boundary layer. This model has been shown by Hunt (1984) to provide a good description of the turbulent structure in the lower part of the atmospheric boundary layer, where the turbulence impinges on the ground. Here we match the turbulence to wave motions in the stratified layer. Townsend (1966) and Stull (1976) calculated the wave motions above a convective layer, but simply assumed the form of the vertical velocity fluctuations at the interface. They did not attempt to *match* the convective turbulence to the wave motion. The data were not then available for any detailed test of the theory.

2. Theory and analysis

2.1. *Assumptions, equations and general solution*

The structure we are considering is shown in figure 2(*a*). Both the turbulent and stratified layers are assumed to be travelling at a constant mean velocity which may or may not be zero. The turbulent layer is assumed to be neutral, and the stratified layer has constant buoyancy frequency N.

2.1.1. *Turbulent region*

In this region the assumptions are similar to those of Hunt (1984). In the interior of the layer the turbulence is assumed to be homogeneous and specified by the energy-spectrum tensor

$$\Phi_{ij}^{(\mathrm{H})}(\boldsymbol{\kappa}) = \iiint_{-\infty}^{\infty} \overline{u_i(x+r)\, u_j(x)}\, \mathrm{e}^{-\mathrm{i}\boldsymbol{\kappa}\cdot\boldsymbol{r}}\, \mathrm{d}\boldsymbol{r}$$

(Batchelor 1953), where u_i, u_j are fluctuating velocities. The observations in the

atmospheric boundary layer by Caughey & Palmer (1979) and Kaimal *et al.* (1976) show that the energy dissipation rate ϵ is approximately constant with height. Hence assuming

$$\frac{\partial \epsilon}{\partial z} = 0, \tag{2.1a}$$

and since $\epsilon = \nu(\overline{\omega^2} - \mathrm{d}^2\overline{q^2}/\mathrm{d}z^2)$, where the vorticity† $\boldsymbol{\omega} = \boldsymbol{\nabla} \times \boldsymbol{u}$ and $q^2 = \overline{u_1^2} + \overline{u_2^2} + \overline{u_3^2}$, then, as the Reynolds number $u_{\mathrm{H}} L_{\mathrm{H}}/\nu \to \infty$,

$$\epsilon = \nu\overline{\omega^2}. \tag{2.1b}$$

So, from (2.1*a*),

$$\frac{\partial \overline{\omega^2}}{\partial z} = 0 \tag{2.1c}$$

and the distortion of the small scales of turbulence is irrotational.

Since the flow is incompressible, the simplest solution satisfying (2.1*a*) is

$$\boldsymbol{u} = \boldsymbol{u}^{(\mathrm{H})} + \boldsymbol{u}^{(\mathrm{S})}, \tag{2.1d}$$

where $\boldsymbol{u}^{(\mathrm{S})}$ is an irrotational field and $\boldsymbol{u}^{(\mathrm{H})}$ is a homogeneous turbulence field. (Note that the superscript (H) is used to denote a variable function in the homogeneous region whereas subscript H is used to denote a constant.)

From (2.1*d*) we have

$$\boldsymbol{u} = \boldsymbol{u}^{(\mathrm{H})} - \boldsymbol{\nabla}\phi, \tag{2.1e}$$

where

$$\nabla^2\phi = 0. \tag{2.1f}$$

Linear equations identical with (2.1*e*) and (2.1*f*) are obtained if the vorticity equation describing the turbulent motion is linearized, as shown by Hunt (1984). He also discusses the nonlinear distortion of turbulent velocity which we have ignored in this analysis. This was estimated to have only a small effect on the vertical fluctuations, but to increase the horizontal fluctuations through stretching of the smaller eddies by the large eddies.

2.1.2. *Stratified region* $z > 0$

In this region it is also assumed that we can neglect nonlinear terms. Then, making the Boussinesq approximation and taking coordinates moving with the mean flow, the equation for the vertical velocity component w‡ is

$$\frac{\partial^2}{\partial t^2}(\nabla^2 w) + N^2\left(\frac{\partial^2}{\partial x^2} + \frac{\partial^2}{\partial y^2}\right)w = 0. \tag{2.2a}$$

Assuming incompressibility, the horizontal components can then be expressed in terms of w by

$$\rho\frac{\partial^2 w}{\partial z\,\partial t} = \left(\frac{\partial^2}{\partial x^2} + \frac{\partial^2}{\partial y^2}\right)p, \tag{2.2b}$$

$$\rho\frac{\partial u}{\partial t} + \frac{\partial p}{\partial x} = 0, \quad \rho\frac{\partial v}{\partial t} + \frac{\partial p}{\partial y} = 0, \tag{2.2c}$$

† In this section (2.1.1) ω is used to denote the magnitude of the vorticity; in all other sections it is used to represent the frequency of wave motions.

‡ For the fluctuating velocities we use either u_1, u_2, u_3 or u, v, w depending on which expressions are the most convenient.

where ρ is the mean density and p the pressure perturbation. By means of (2.2a) we obtain the Fourier transform of the vertical velocity $\hat{w}$

$$\frac{\mathrm{d}^2\hat{w}}{\mathrm{d}z^2}+\left(\frac{N^2}{\omega^2}-1\right)(\kappa_1^2+\kappa_2^2)\,\hat{w}=0, \tag{2.3a}$$

where

$$w=\iiint_{-\infty}^{\infty}\hat{w}\,\mathrm{e}^{\mathrm{i}(\kappa_1 x+\kappa_2 y-\omega t)}\,\mathrm{d}\kappa_1\,\mathrm{d}\kappa_2\,\mathrm{d}\omega \tag{2.3b}$$

and ω is the intrinsic frequency of the wave motion. As $z\to\infty$ the conditions are the outward radiation of energy for $\omega < N$ and that $w\to 0$ for $\omega > N$.

2.1.3. *At the interface*

The kinematic condition is that w is continuous at the interface. Also assuming that the pressure is continuous, from the dynamical equations it follows that $\partial w/\partial z$ is continuous (Goldstein 1931).

The system of equations is closed by defining the joint wavenumber and frequency spectrum in homogeneous turbulence:

$$\chi_{ij}^{(\mathrm{H})}(\boldsymbol{\kappa},\omega)=\iiint_{-\infty}^{\infty}\overline{u_i(\boldsymbol{x},\tau)\,u_j(\boldsymbol{x}+\boldsymbol{r},\tau+t)}\,\mathrm{e}^{-\mathrm{i}(\boldsymbol{\kappa}.\boldsymbol{r}-\omega t)}\,\mathrm{d}\boldsymbol{r}\,\mathrm{d}t. \tag{2.4}$$

In homogeneous turbulence there have not even been measurements of the Eulerian frequency spectrum

$$\phi_{ij}^{(\mathrm{H})}(\omega)=\int_{-\infty}^{\infty}\overline{u_i(\tau)\,u_j(\tau+t)}\,\mathrm{e}^{-\mathrm{i}\omega t}\,\mathrm{d}t,$$

let alone $\chi_{ij}^{(\mathrm{H})}(\boldsymbol{\kappa},\omega)$, so we use a plausible argument due to Tennekes (1975) to propose an approximate form for $\chi_{ij}^{(\mathrm{H})}(\boldsymbol{\kappa},\omega)$ in terms of the specified wavenumber spectrum of the homogeneous turbulence $\Phi_{ij}^{(\mathrm{H})}(\boldsymbol{\kappa})$.

There are two main causes for the time variation in the velocity at a point moving with the *mean flow*: the change of velocity of a fluid element (which occurs in the Lagrangian timescale τ_{L}) and the random velocity of advection of fluid elements by the most energetic eddies (on a timescale l/u_{H}, where l is the lengthscale of the advected energy and u_{H} the velocity scale of the turbulence). The former process leads to a 'Lagrangian' frequency spectrum proportional to $\epsilon\omega^{-2}$ while the latter leads to an 'Eulerian' frequency spectrum

$$\phi_{ij}(\omega)=A\epsilon^{\frac{2}{3}}u_{\mathrm{H}}^{\frac{2}{3}}\,\omega^{-\frac{5}{3}}, \tag{2.5a}$$

where A is constant for a given i, j.

In physical terms the result of the use of the 'Lagrangian' spectrum in the analysis would correspond to a model of waves being produced by eddies rising or falling, whereas the result using the Eulerian spectrum corresponds to a model of waves being produced by eddies randomly moving horizontally along the interface (figure 2b). The analysis presented here makes use of the Eulerian spectrum since it is more energetic at moderate-to-high frequencies ($\omega > u_{\mathrm{H}}/L_{\mathrm{H}}$) because the energy at frequency ω is largely being induced by eddies of wavenumber $|\boldsymbol{\kappa}|\approx\omega/u_{\mathrm{H}}$. Making use of the Eulerian spectrum (2.5a) the joint wavenumber and frequency spectrum should have the approximate form

$$\chi_{ij}^{(\mathrm{H})}(\boldsymbol{\kappa},\omega)=\Phi_{ij}^{(\mathrm{H})}(\boldsymbol{\kappa})\,\delta(\omega-u_{\mathrm{H}}\,k), \tag{2.5b}$$

where $k=|\boldsymbol{\kappa}|$. In reality the energy at frequency ω is associated with a range of wavenumbers centred on ω/u_{H} (e.g. Townsend 1966; Stull 1976) but, without any

measurements to indicate this range, it is simplest to specify that all the energy of frequency ω is associated with the wavenumber k. This implies the delta-function form of the spectrum (2.5*b*). For example, assuming that the energy-spectrum tensor has the form suggested by von Kármán (see §2.3) and taking $i = j = 1$, then, when $k \gg L_{\mathrm{H}}^{-1}$,

$$\Phi_{11}^{(\mathrm{H})}(k) = \frac{A' \epsilon^{\frac{2}{3}} k_{23}^2}{k^{\frac{17}{3}}}, \tag{2.5c}$$

where $$A' = \frac{55}{36\pi}\left(\frac{\Gamma(\frac{5}{6})}{\Gamma(\frac{1}{3})}\right)^{\frac{5}{3}}, \quad k_{ij}^2 = \kappa_i^2 + \kappa_j^2.$$

Then from (2.5*b*) and (2.5*c*)

$$\phi_{11}^{(\mathrm{H})}(\omega) = \iiint_{-\infty}^{\infty} \Phi_{11}^{(\mathrm{H})}(\boldsymbol{\kappa})\, \delta(\omega - u_{\mathrm{H}} k)\, \mathrm{d}\boldsymbol{\kappa} \tag{2.5d}$$

and, at high frequencies, $\omega/u_{\mathrm{H}} \gg L_{\mathrm{H}}^{-1}$, the frequency spectrum of u_1 in homogeneous turbulence is given by

$$\left.\begin{aligned} \phi_{11}^{(\mathrm{H})}(\omega) &= \iiint_{-\infty}^{\infty} A' \epsilon^{\frac{2}{3}} \frac{k_{23}^2}{k^{\frac{17}{3}}} \delta(\omega - u_{\mathrm{H}} k)\, \mathrm{d}\boldsymbol{\kappa} \\ &= (\tfrac{4}{3}\pi)\, A' \epsilon^{\frac{2}{3}} u_{\mathrm{H}}^{\frac{2}{3}}\, \omega^{-\frac{5}{3}}. \end{aligned}\right\} \tag{2.5e}$$

This shows that (2.5*b*) is consistent with (2.5*a*).

In the analysis that follows, we shall use a slightly modified form of (2.5*b*) so that the integrals can be calculated more easily, viz.

$$\chi_{ij}^{(\mathrm{H})}(\boldsymbol{\kappa}, \omega) = \Phi_{ij}^{(\mathrm{H})}(\boldsymbol{\kappa})\, \delta(\omega - u_{\mathrm{H}} k_{12}). \tag{2.5f}$$

The wavenumber k has been replaced by the horizontal wavenumber k_{12}. The effect of this modification on the solution has been calculated for the case of a delta-function form of isotropic turbulence (see §2.3). This approximation introduces a small numerical factor in the magnitude; it does not affect the form of the results. In using (2.5*f*) to calculate $\chi_{ij}^{(\mathrm{H})}(\boldsymbol{\kappa}, \omega)$ in terms of $\Phi_{ij}^{(\mathrm{H})}(\boldsymbol{\kappa})$, we are assuming also that the horizontal velocity fluctuations near the interface are of order u_{H}. This assumption is justified *a posteriori* since analysis at the interface shows that $1.5u_{\mathrm{H}}^2 \geqslant \overline{u_i^2} \geqslant u_{\mathrm{H}}^2$, where $i = 1$ or 2.

2.1.4. *Method of solution*

The procedure is to first solve the x, y, t Fourier transform of the Laplace equation for the velocity potential ϕ in the turbulent region (2.1*f*)

$$\frac{\partial^2 \hat{\phi}}{\partial z^2} - k_{12}^2 \hat{\phi} = 0. \tag{2.6a}$$

Using (2.1*e*) an expression can then be obtained for the x, y, t Fourier transform of the vertical velocity ($\hat{w}$) in the turbulent region. This is described in terms of the x, y, z, t Fourier transform, $S_3^{(\mathrm{H})}(\boldsymbol{k}, \omega)$, of the vertical velocity $w^{(\mathrm{H})}$ in the homogeneous turbulence, where

$$S_i^{(\mathrm{H})}(\boldsymbol{\kappa}, \omega) = \iiint_{-\infty}^{\infty} u_i(\boldsymbol{r}, t)\, \mathrm{e}^{-(\boldsymbol{\kappa}.\boldsymbol{r} - \omega t)}\, \mathrm{d}\boldsymbol{r}\, \mathrm{d}t. \tag{2.6b}$$

An expression for $\hat{w}(\kappa_1, \kappa_2, z, \omega)$ in the stably stratified region is then obtained using (2.3*a*) and making use of the upper boundary conditions (§2.1.2).

Each of the two expressions for $\hat{w}$ contains one unknown coefficient which is now

calculated by matching the two expressions for $\hat{w}$ at the interface, making use of the boundary conditions §2.1.3 that w and $\partial w/\partial z$ are continuous at the interface. From the forms for $\hat{w}$ we obtain forms for $\hat{u}$, $\hat{v}$ in both regions using (2.1 e), (2.2b) and (2.2c). It is convenient to use the following scaling:

$$N^* = \frac{NL_H}{u_H}, \quad \omega^* = \frac{\omega L_H}{u_H}, \quad \kappa^* = \kappa L_H, \quad \boldsymbol{u}^* = \frac{\boldsymbol{u}}{u_H},$$

where the bars denote non-dimensional quantities and, $L_H = L_x^{(H)}$, the longitudinal integral scale of the homogeneous turbulence. For brevity we omit the asterisks. All the following expressions in this section are non-dimensional.

In the turbulent region ($z \leqslant 0^-$)

$$\hat{w}(\kappa_1, \kappa_2, z, \omega) = \int_{-\infty,\, \omega<N}^{\infty} S_3^{(H)} \left[e^{i\kappa_3 z} + \frac{((N^2/\omega^2)-1)\, e^{k_{12}z}}{1-i((N^2/\omega^2)-1)^{\frac{1}{2}}} \right] d\kappa_3 + \int_{-\infty,\, \omega>N}^{\infty} S_3^{(H)} \left[e^{i\kappa_3 z} - \frac{(1-N^2/\omega^2)^{\frac{1}{2}}\, e^{k_{12}z}}{1+(1-N^2/\omega^2)^{\frac{1}{2}}} \right] d\kappa_3, \quad (2.7a)$$

$$\hat{u}_j(\kappa_1, \kappa_2, z, \omega) = \int_{-\infty,\, \omega<N}^{\infty} \left[S_j^{(H)}\, e^{i\kappa_3 z} + \frac{\kappa_j}{k_{12}} \left(\frac{N^2}{\omega^2} - 1 \right)^{\frac{1}{2}} \frac{S_3^{(H)}\, e^{k_{12}z}}{1+i(N^2/\omega^2-1)^{\frac{1}{2}}} \right] d\kappa_3 + \int_{-\infty,\, \omega>N}^{\infty} \left[S_j^{(H)}\, e^{i\kappa_3 z} - \frac{i\kappa_j}{k_{12}} \left(1 - \frac{N^2}{\omega^2} \right)^{\frac{1}{2}} \frac{S_3^{(H)}\, e^{k_{12}z}}{1+(1-N^2/\omega^2)^{\frac{1}{2}}} \right] d\kappa_3, \quad (2.7b)$$

where $j = 1$ or 2. In each case the first or second integral contributes depending on whether $\omega < N$ or $\omega > N$.

In the stratified region ($z \geqslant 0^+$)†

$$\hat{\boldsymbol{u}}(\kappa_1, \kappa_2, z, \omega) = \int_{-\infty,\, \omega<N}^{\infty} \left(\frac{-\kappa_1}{k_{12}} \left(\frac{N^2}{\omega^2} - 1 \right)^{\frac{1}{2}}, \frac{-\kappa_2}{k_{12}} \left(\frac{N^2}{\omega^2} - 1 \right)^{\frac{1}{2}}, 1 \right) \frac{S_3^{(H)} \exp\left[i((N^2/\omega^2)-1)^{\frac{1}{2}} k_{12} z \right]}{1-i((N^2/\omega^2)-1)^{\frac{1}{2}}} d\kappa_3 + \int_{-\infty,\, \omega>N}^{\infty} \left(\frac{i\kappa_1}{k_{12}} \left(1 - \frac{N^2}{\omega^2} \right)^{\frac{1}{2}}, \frac{i\kappa_2}{k_{12}} \left(1 - \frac{N^2}{\omega^2} \right)^{\frac{1}{2}}, 1 \right) \frac{S_3^{(H)} \exp\left[-(1-N^2/\omega^2)^{\frac{1}{2}} \right] k_{12} z}{1+(1-N^2/\omega^2)^{\frac{1}{2}}} d\kappa_3. \quad (2.8)$$

We can now obtain expressions for the one-dimensional spectra defined as

$$\Theta_{ij}(\kappa_1) = \int_{-\infty}^{\infty} \int_{-\infty}^{\infty} \Phi_{ij}(\boldsymbol{\kappa})\, d\kappa_2\, d\kappa_3$$

from

$$\Theta_{ii}(\kappa_1) = \int_{-\infty}^{\infty} \overline{\hat{u}_i^{\dagger} \hat{u}_i}\, d\kappa_2 \quad (i = 1, 2 \text{ or } 3) \quad (2.9a)$$

and also using

$$\overline{S_i^{(H)\dagger}(\boldsymbol{\kappa}, \omega)\, S_j^{(H)}(\boldsymbol{\kappa}', \omega')} = \chi_{ij}^{(H)}(\boldsymbol{\kappa}, \omega)\, \delta(\boldsymbol{\kappa} - \boldsymbol{\kappa}')\, \delta(\omega - \omega'), \quad (2.9b)$$

where † denotes the complex conjugate, the u_i are defined in (2.7) (2.8), and $\chi_{ij}^{(H)}(\boldsymbol{\kappa}, \omega) = \Phi_{ij}^{(H)}(\boldsymbol{\kappa})\, \delta(\omega - u_H k_{12})$, as defined in (2.5$f$). It is now apparent why it is necessary to obtain a form for the joint wavenumber and frequency spectrum in the

† The superscripts $-$, $+$ show whether we are referring either to the turbulent region or to the stratified region at the interface. A distinction is necessary since u and v are discontinuous there.

homogeneous turbulence. In the turbulent region ($z \leqslant 0^-$), the one-dimensional spectrum of the vertical fluctuations is given by

$$\Theta_{33}(\kappa_1, z, N) = 2\int_{\substack{-\infty \\ k_{12}<N}}^{\infty}\int_0^{(N^2-\kappa_1^2)^{\frac{1}{2}}}\left\{2\,\mathrm{e}^{k_{12}z}\left(\left(1-\frac{N^2}{k_{12}^2}\right)\cos\kappa_3 z+\left(1-\frac{N^2}{k_{12}^2}\right)^{\frac{1}{2}}\sin\kappa_3 z\right)\right.$$
$$\left.+\left(1-\frac{k_{12}^2}{N^2}\right)\mathrm{e}^{2k_{12}z}\right\}\Phi_{33}^{(\mathrm{H})}(\boldsymbol{\kappa})\,\mathrm{d}\kappa_2\,\mathrm{d}\kappa_3$$
$$+2\int_{\substack{-\infty \\ k_{12}>N}}^{\infty}\int_{(N^2-\kappa_1^2)^{\frac{1}{2}}}^{\infty}\left\{\frac{-2\,\mathrm{e}^{k_{12}z}\left(1-\frac{N^2}{k_{12}^2}\right)^{\frac{1}{2}}\cos\kappa_3 z}{\left(1+\left(1-\frac{N^2}{k_{12}^2}\right)^{\frac{1}{2}}\right)^2}\right.$$
$$\left.+\frac{\left(1-\frac{N^2}{k_{12}^2}\right)\mathrm{e}^{2k_{12}z}}{\left(1+\left(1-\frac{N^2}{k_{12}^2}\right)^{\frac{1}{2}}\right)^2}\right\}\Phi_{33}(\boldsymbol{\kappa})\,\mathrm{d}\kappa_2\,\mathrm{d}\kappa_3+\Theta_{33}^{(\mathrm{H})}(\kappa_1). \tag{2.10a}$$

The spectra of the horizontal components, $j = 1$ or 2 are

$$\Theta_{jj}(\kappa_1, z, N) = \Theta_{jj}^{(\mathrm{H})}(\kappa_1)+2\int_{\substack{-\infty \\ k_{12}<N}}^{\infty}\int_0^{(N^2-\kappa_1^2)^{\frac{1}{2}}}\left\{\frac{2\kappa_j}{k_{12}}\,\mathrm{e}^{k_{12}z}\left(\left(\frac{k_{12}^2}{N^2}-1\right)\sin\kappa_3 z\right.\right.$$
$$\left.-\frac{k_{12}^2}{N^2}\left(\frac{N^2}{k_{12}^2-1}\right)^{\frac{1}{2}}\cos\kappa_3 z\right)\Phi_{j3}^{(\mathrm{H})}(\boldsymbol{\kappa})+\frac{\kappa_j^2}{N^2}\left(\frac{N^2}{k_{12}^2}-1\right)\mathrm{e}^{2k_{12}z}\,\Phi_{33}^{(\mathrm{H})}(\boldsymbol{\kappa})\Big\}\,\mathrm{d}\kappa_2\,\mathrm{d}\kappa_3$$
$$+2\int_{\substack{-\infty \\ k_{12}>N}}^{\infty}\int_{(N^2-\kappa_1^2)^{\frac{1}{2}}}^{\infty}\left\{\frac{-2\kappa_j}{k_{12}}\frac{\mathrm{e}^{k_{12}z}\left(1-\frac{N^2}{k_{12}^2}\right)^{\frac{1}{2}}}{\left(1+\left(1-\frac{N^2}{k_{12}^2}\right)^{\frac{1}{2}}\right)}\sin\kappa_3 z\,\Phi_{j3}^{(\mathrm{H})}(\boldsymbol{\kappa})\right.$$
$$\left.+\frac{\kappa_j^2}{k_{12}^2}\left(1-\frac{N^2}{k_{12}^2}\right)\frac{\mathrm{e}^{k_{12}z}}{\left(1+\left(1-\frac{N^2}{k_{12}^2}\right)^{\frac{1}{2}}\right)^2}\Phi_{33}^{(\mathrm{H})}(\boldsymbol{\kappa})\quad\mathrm{d}\kappa_2\,\mathrm{d}\kappa_3.\right\} \tag{2.10b}$$

In each case both integrals contribute: the former when $k_{12} < N$, the latter when $k_{12} > N$.

In the stratified region ($z \geqslant 0^+$),

$$\Theta_{33}(\kappa_1, z, N) = 2\int_{\substack{-\infty \\ k_{12}>N}}^{\infty}\int_0^{(N^2-\kappa_1^2)^{\frac{1}{2}}}\frac{k_{12}^2}{N^2}\,\Phi_{33}^{(\mathrm{H})}(\boldsymbol{\kappa})\,\mathrm{d}\kappa_2\,\mathrm{d}\kappa_3$$
$$+2\int_{\substack{-\infty \\ k_{12}<N}}^{\infty}\int_{(N^2-\kappa_1^2)^{\frac{1}{2}}}^{\infty}\frac{\exp\left[-2\left(1-\frac{N^2}{k_{12}^2}\right)^{\frac{1}{2}}k_{12}z\right]}{\left(1+\left(1-\frac{N^2}{k_{12}^2}\right)^{\frac{1}{2}}\right)^2}\Phi_{33}^{(\mathrm{H})}(\boldsymbol{\kappa})\,\mathrm{d}\kappa_2\,\mathrm{d}\kappa_3, \tag{2.11a}$$

$$\Theta_{jj}(\kappa_1, z, N) = 2\int_{\substack{-\infty \\ \kappa_{12}<N}}^{\infty} \int_0^{(N^2-\kappa_1^2)^{\frac{1}{2}}} \frac{\kappa_j^2}{N^2}\left(\frac{N^2}{k_{12}^2}-1\right)\Phi_{33}^{(\mathrm{H})}(\boldsymbol{\kappa})\,\mathrm{d}\kappa_2\,\mathrm{d}\kappa_3$$
$$+\int_{-\infty}^{\infty}\int_{(N^2-\kappa_1^2)^{\frac{1}{2}}}^{\infty} \frac{\kappa_j^2}{k_{12}^2}\left(1-\frac{N^2}{k_{12}^2}\right)\frac{\exp\left[-\left(1-\frac{N^2}{k_{12}^2}\right)^{\frac{1}{2}} k_{12} z\right]}{\left(1+\left(1-\frac{N^2}{k_{12}^2}\right)^{\frac{1}{2}}\right)^2}\Phi_{33}^{(\mathrm{H})}(\boldsymbol{\kappa})\,\mathrm{d}\kappa_2\,\mathrm{d}\kappa_3, \tag{2.11b}$$

$j = 1$ or 2 (i.e. no summation). The former integral for each velocity component represents the spectrum of propagating gravity waves, the latter the spectrum of evanescent waves.

2.2. *General results for any spectra of the homogeneous turbulence*

A number of results can be obtained without specifying the turbulence spectrum. First we find the discontinuity in the spectra of the horizontal velocity components at the interface:

$$\Theta_{jj}(\kappa_1, z = 0^-) = \Theta_{jj}(\kappa_1, z = 0^+) + \Theta_{jj}^{(\mathrm{H})}(\kappa_1), \tag{2.12}$$

where $j = 1$ or 2. Thus there is a discontinuity by an amount $\Theta_j^{(\mathrm{H})}(\kappa_1)$, independent of the buoyancy frequency N. At low horizontal wavenumbers since $\boldsymbol{u}^{(\mathrm{S})} = -\nabla\phi$, then

$$\Theta_{11}(\kappa_1 = 0, z = 0^-) = \Theta_{11}^{(\mathrm{H})}(\kappa_1 = 0), \quad \Theta_{22}(\kappa_2 = 0, z = 0^-) = \Theta_{22}^{(\mathrm{H})}(\kappa_2 = 0) \tag{2.13a}$$

and

$$\Theta_{11}(\kappa_1 = 0, z = 0^+) = \Theta_{22}(\kappa_2 = 0, z = 0^+) = 0. \tag{2.13b}$$

Thus in the low-wavenumber limit the spectra of the horizontal components are independent of N and z.

In the limit of large stratification ($N \to \infty$) solutions for Θ_{jj} ($j = 1, 2, 3$) in the turbulent region reduce to equations (2.53–2.55) of Hunt & Graham (1978) for turbulence near a rigid surface. Thus in this limit the turbulence below the interface behaves as if it were confined by a rigid surface.

In the stratified region, from (2.11) it follows that the gravity-wave parts of the spectra are independent of z. When $N \to \infty$ and $z \geqslant 0^+$

$$\Theta_{33}(\kappa_1) = 0, \tag{2.14a}$$

$$\Theta_{jj}(\kappa_1) = \int_{-\infty}^{\infty}\int_{-\infty}^{\infty} \frac{\kappa_j^2}{k_{12}^2}\Theta_{33}^{(\mathrm{H})}(\boldsymbol{\kappa})\,\mathrm{d}\kappa_2\,\mathrm{d}\kappa_3 \quad (j = 1 \text{ or } 2) \tag{2.14b}$$

and

$$\overline{u_1^2} = \overline{u_2^2} = 0.5u_{\mathrm{H}}^2. \tag{2.14c}$$

In the limit of zero stratification $N \to 0$, the solution in the non-turbulent region ($z \geqslant 0^+$) is similar to Phillips' (1955) solution for irrotational fluctuations outside a turbulent region. However Phillips did not consider any feedback between the two layers. He used only the kinematic boundary condition at the interface and assumed that the turbulence was undistorted by the fluid in the irrotational region, whereas the absence of rotational motion above $z = 0$ must reduce the velocity fluctuations below $z = 0$. The difference between these solutions only affects the magnitude of the irrotational fluctuations in terms of the magnitude of the homogeneous turbulence; it does not affect the relative magnitudes of the different components of the irrotational velocity fluctuations. Our solution gives

$$\left.\begin{aligned} \overline{u_3^2}(z = 0) &= 0.25u_{\mathrm{H}}^2, \\ \Theta_{33}(\kappa_1, z = 0) &= \tfrac{1}{4}\Theta_{33}^{(\mathrm{H})}(\kappa_1), \end{aligned}\right\} \tag{2.15}$$

whereas in Phillips' (1955) solution

$$\left.\begin{aligned}\overline{u_3^2}(z=0) &= u_{\mathrm{H}}^2,\\ \Theta_{33}(\kappa_1, z=0) &= \Theta_{33}^{(\mathrm{H})}(\kappa_1).\end{aligned}\right\} \tag{2.16}$$

Both results are independent of the form of $\Theta_{ij}^{(\mathrm{H})}(\boldsymbol{\kappa})$ and both result in the mean square of the horizontal velocity components being half that of the vertical components, i.e.

$$\overline{u_j^2} = 0.5\overline{u_3^2} \quad (z \geqslant 0^+, j = 1 \text{ or } 2). \tag{2.17}$$

2.3. *Results for delta-function spectra*

To understand how different eddy sizes of the homogeneous turbulence interact with the stable layer, we first consider some examples of isotropic energy-spectrum tensors where all the energy is at a single wavenumber, i.e. $|\boldsymbol{\kappa}| = k_{\mathrm{w}}$. Essentially these represent spectra of isotropic simple waves (Tennekes & Lumley 1972, p. 254). In this case

$$\Phi_{ij}^{(\mathrm{H})}(\boldsymbol{\kappa}) = \frac{E(k)}{4\pi k^4}(k^2\delta_{ij} - \kappa_i\kappa_j) \tag{2.18}$$

(Batchelor 1953), where we take the energy spectra to be $E(k) = \frac{3}{2}\delta(k-1)$, and $\boldsymbol{\kappa}$ is normalized on k_{w}. Thence

$$\Theta_{11}^{(\mathrm{H})}(\kappa_1) = \tfrac{3}{4}(1-\kappa_1^2) \quad (\kappa_1 \leqslant 1); \quad \Theta_{11}^{(\mathrm{H})}(\kappa_1) = 0 \quad (\kappa_1 > 1) \tag{2.19a}$$

$$\Theta_{22}^{(\mathrm{H})}(\kappa_1) = \Theta_{33}^{(\mathrm{H})}(\kappa_1) = \tfrac{3}{8}(1+\kappa_1^2) \quad (\kappa_1 \leqslant 1); \quad \Theta_{22}^{(\mathrm{H})}(\kappa_1) = \Theta_{33}^{(\mathrm{H})}(\kappa_1) = 0 \quad (\kappa_1 > 1). \tag{2.19b}$$

Expressions for the one-dimensional spectra and variances near the interface obtained using (2.10) are presented below for $z \geqslant 0^+$ and $N \geqslant 1$, and for $N = 0$ on $z = 0$. N is normalized by k_{w} and u_{H}.

(*a*) $N \geqslant 1$, $z \geqslant 0^+$:

$$\Theta_{33}(\kappa_1) = \frac{3}{16N^2}(\tfrac{3}{2}(1+\kappa_1^4)+\kappa_1^2) \tag{2.20a}$$

$$\Theta_{11}(\kappa_1) = \frac{3\kappa_1^2}{4N^2}(N^2 - \tfrac{1}{2}(1+\kappa_1^2)), \tag{2.20b}$$

$$\Theta_{22}(\kappa_1) = \frac{3}{4N^2}(1-\kappa_1^2)(\tfrac{1}{2}N^2 - \tfrac{1}{8}\kappa_1^2 - \tfrac{3}{8}), \tag{2.20c}$$

with variances

$$\frac{\overline{u_3^2}}{u_{\mathrm{H}}^2} = \frac{4}{5}\frac{1}{N^2}, \tag{2.20d}$$

$$\frac{\overline{u_1^2}}{u_{\mathrm{H}}^2} = \frac{\overline{u_2^2}}{u_{\mathrm{H}}^2} = \frac{1}{2} - \frac{2}{5}\frac{1}{N^2}. \tag{2.20e}$$

(*b*) $N = 0$, $z = 0$:

$$\Theta_{33}(\kappa_1) = \tfrac{1}{4}\Theta_{33}^{(\mathrm{H})}(\kappa_1); \quad \Theta_{22}(\kappa_1) = \tfrac{1}{8}\Theta_{33}^{(\mathrm{H})}(\kappa_1); \quad \Theta_{11}(\kappa_1) = \tfrac{3}{32}(1-\kappa_1^2); \tag{2.21a}$$

$$\overline{u_3^2} = 0.25u_{\mathrm{H}}^2; \quad \overline{u_1^2} = \overline{u_2^2} = 0.125u_{\mathrm{H}}^2. \tag{2.21b}$$

For the case discussed in this section of isotropic simple waves in the interior of the 'turbulent region', the spectra and variances can also be calculated easily for the form

of wavenumber and frequency spectrum $\chi_{ij}^{(\mathrm{H})}(\boldsymbol{\kappa},\omega) = \Theta_{ij}^{(\mathrm{H})}\,\delta(\omega - u_{\mathrm{H}}\,k)$ (2.5b). Such calculations can be used to examine the effect of replacing the wavenumber k with k_{12} in the calculations in the following sections in which more realistic turbulent spectra are specified.

On $z \geqslant 0^+$, $N \geqslant 1$ using (2.5b)

$$\Theta_{33}(K_1) = \frac{3}{8}\frac{1+\kappa_1^2}{N^2}, \quad \Theta_{11}(\kappa_1) = \frac{3}{4}\frac{\kappa_1^2}{N^2}(N^2-1), \quad \Theta_{22}(\kappa_1) = \tfrac{3}{8}(1-\kappa_1^2)(1-1/N^2), \quad (2.22a)$$

with variances

$$\frac{\overline{u_3^2}}{u_{\mathrm{H}}^2} = \frac{1}{N^2}, \quad \frac{\overline{u_1^2}}{u_{\mathrm{H}}^2} = \frac{\overline{u_2^2}}{u_{\mathrm{H}}^2} = \frac{1}{2}\left(1-\frac{1}{N^2}\right). \quad (2.22b)$$

On $z = 0$, $N = 0$ using (2.5b), the solutions are identical with those of (b) above.

The spectra and variances for both forms of the wavenumber and frequency spectrum are shown in figures 3 and 4. The difference between the solutions for the two forms of $\chi_{ij}^{(\mathrm{H})}(\boldsymbol{\kappa},\omega)$ is negligible except where $N \approx 1$ (in dimensional terms) when the difference is small. In this case, using $\omega = u_{\mathrm{H}}\,k$ (2.5b) results in no damping of the vertical motion at the interface, whilst using $\omega = u_{\mathrm{H}}\,k_{12}$ (2.5e), there is some damping ($(\overline{u_3^2}/u_{\mathrm{H}}^2)(z=0) = \frac{4}{5}$) and consequently a small amplification in the horizontal components. The difference occurs because using $\omega = u_{\mathrm{H}}\,k_{12}$ results in isotropic waves of wavenumber k_{w} contributing to all frequencies $\omega \leqslant u_{\mathrm{H}}\,k_{\mathrm{w}}$ and frequencies $\omega < u_{\mathrm{H}}\,k_{\mathrm{w}}$ are damped by the stratification. However, when $\omega = u_{\mathrm{H}}\,k$ the single frequency $\omega = u_{\mathrm{H}}\,k_{\mathrm{w}}$ contributes.

For both forms of $\chi_{ij}^{(\mathrm{H})}(\boldsymbol{\kappa},\omega)$ when $N < 1$ ($= 0$ in our case) and $N \gg 1$ vertical motions are much reduced. The longitudinal spectra show maximum excitation at the highest frequencies excited, $\kappa_1/k_{\mathrm{w}} \approx 1$, while the transverse fluctuations are greatest at low frequencies, which is a similar result to that of Hunt & Graham (1978) for zero-shear turbulence near a wall. The kinetic energy of the wave motion in the stratified layer is independent of N for a given k_{w}, when, in dimensional terms, $N > u_{\mathrm{H}}\,k_{\mathrm{w}}$; viz.

$$q^2(z>0) = \tfrac{1}{3}q_{\mathrm{H}}^2, \quad (2.23a)$$

$$q^2(z=0^-) = q_{\mathrm{H}}^2. \quad (2.23b)$$

2.4. *Forms of the energy-spectrum tensor*

In order to obtain specific results for the changes in the variances and spectra near the interface, the integrals in (2.9)–(2.12) require specification of the energy-spectrum tensor $\Phi_{ij}^{(\mathrm{H})}(\boldsymbol{\kappa})$ of the homogeneous isotropic turbulence. We consider two different expressions, which have the same general form, namely

$$\Phi_{ij}^{(\mathrm{H})}(\boldsymbol{\kappa}) = \frac{g_3(k^2\delta_{ij} - \kappa_i\kappa_j)}{(g_2+k^2)^{\mu+2}}, \quad (2.24)$$

and which have one-dimensional spectra given by

$$\Theta_{ij}^{(\mathrm{H})}(\boldsymbol{\kappa}) = \frac{g_1}{(g_2+\kappa_1^2)^{\mu}}. \quad (2.25)$$

In the von Kármán form $\mu = \frac{5}{6}$, $g_1 = g_2^{\frac{5}{6}}/\pi = 0.1955$, $g_2 = \pi\Gamma^2(\frac{5}{6})/\Gamma^2(\frac{1}{3}) = 0.558$, $g_3 = 55g_1/36\pi$, whereas the Townsend form requires $\mu = 1$, $g_1 = 1/\pi$, $g_2 = 1$ and $g_3 = 2g_1/\pi$. The von Kármán spectrum generally gives a more accurate representation

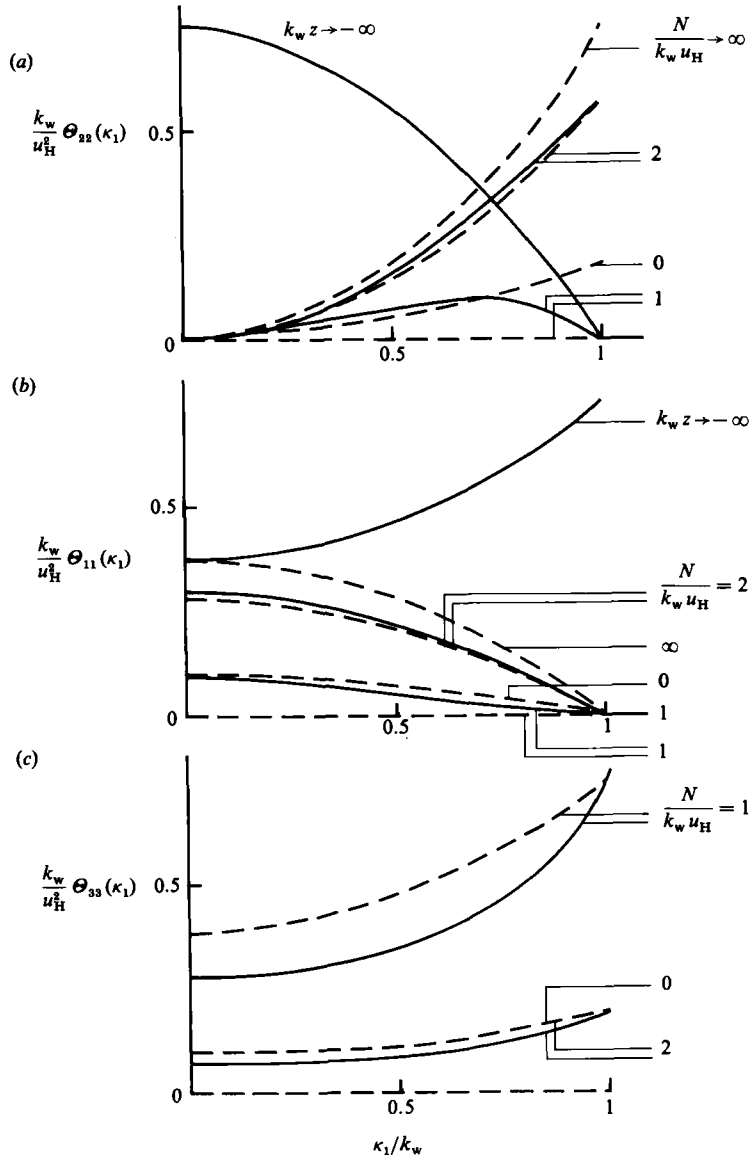

FIGURE 3. Calculated one-dimensional spectra at $z = 0$ and $\kappa_1/\kappa_w \gg 1$ for the case of isotropic simple waves in the free stream ——, $\chi_{ij}^{(H)}(\boldsymbol{\kappa}, \omega) = \Phi_{ij}^{(H)}(\boldsymbol{\kappa})\,\delta(\omega - u_H k_{12})$; – – –, $\chi_{ij}^{(H)}(\boldsymbol{\kappa}, \omega) = \Phi_{ij}^{(H)}(\boldsymbol{\kappa})\,\delta(\omega - u_H k)$: (*a*) longitudinal component, (*b*) transverse component, (*c*) normal component. Where only one curve is shown for a particular value of $N/k_w u_H$, the solutions for each form of $\chi_{ij}^{(H)}(\kappa, \omega)$ are identical.

of turbulence, reducing to the Kolmogorov spectrum $\Theta_{11}^{(H)}(\kappa_1) = g_1/\kappa_1^{\frac{5}{3}}$ for $\kappa_1 \gg g_2$. However, the Townsend spectrum enables the integrals to be calculated more easily. We shall present analytical expressions obtained using the von Kármán spectrum in the main body of the text, whilst expressions obtained using Townsend's spectrum are set out in the Appendix.

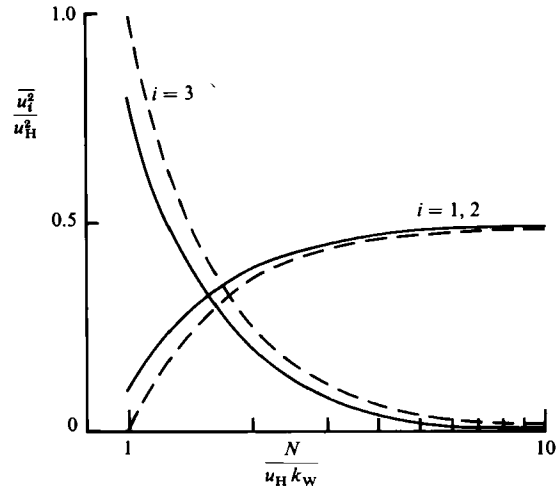

FIGURE 4. Variances at $z = 0$ for isotropic simple waves in the free stream. The notation is that of figure 3.

2.5. *Results for von Kármán and Townsend spectra*

2.5.1. *One-dimensional spectra*

Von Kármán form: For this form of the spectra analytical expressions are obtainable for the limits $\kappa_1 \to 0$ and $N \gg 1$ for $z \geqslant 0^+$. The suffixes g and e refer to the contributions to the spectra from the different frequency ranges:

(i) $\omega < N$ (gravity waves in stratified layers),

(ii) $\omega > N$ (evanescent waves in the stratified layer).

$$\Theta_{33}^{g}(\kappa_1 = 0, z \geqslant 0^+, N \gg 1) = \frac{1}{3}\frac{\gamma}{N^{\frac{5}{3}}}, \tag{2.26a}$$

$$\Theta_{33}^{e}(\kappa_1 = 0, z = 0^+, N \gg 1) = \tfrac{1}{9} I(\tfrac{2}{3})\frac{\gamma}{N^{\frac{5}{3}}}, \tag{2.26b}$$

where

$$\gamma = \frac{8 g_1 \Gamma(\frac{1}{3})}{\pi^{\frac{1}{2}}\Gamma(\frac{5}{6})} \approx 2.097, \tag{2.27a}$$

$$I(q) = \int_0^1 \frac{x^q \, dx}{[1+(1-x^2)^{\frac{1}{2}}]^2}, \quad \text{and} \quad I(\tfrac{2}{3}) \approx 0.226, \tag{2.27b}$$

$$\Theta_{11}^{g}(\kappa_1 = 0, z \geqslant 0^+, N \gg 1) = \Theta_{11}^{e}(\kappa_1 = 0, z = 0^+, N \gg 1) = 0, \tag{2.28a}$$

$$\Theta_{22}^{g}(\kappa_1 = 0, z = 0^+, N \gg 1) = \frac{1}{2\pi} - \frac{2}{5}\frac{\gamma}{N^{\frac{5}{3}}}, \tag{2.28b}$$

$$\Theta_{22}^{e}(\kappa_1 = 0, z = 0^+, N \gg 1) = \frac{8\gamma}{N^{\frac{5}{3}}}(I(\tfrac{2}{3}) - I(\tfrac{8}{3})) \tag{2.28c}$$

$$\approx 0.023/N^{\frac{5}{3}} \quad (\text{since } I(\tfrac{8}{3}) = 0.127).$$

Townsend form: For this form of spectra, (2.10) and (2.11) can be integrated exactly for all κ_1 and for $N < \omega$ and $z \geqslant 0^+$. The analytical expressions are set out in the Appendix.

Computed spectra using both the von Kármán and Townsend forms are plotted as functions of z and N in figure 5. Note how, at $z = 0$, as N increases the value of κ_1 for which $\Theta_{33}(\kappa_1)$ is a maximum slightly increases, a result of the fact that the

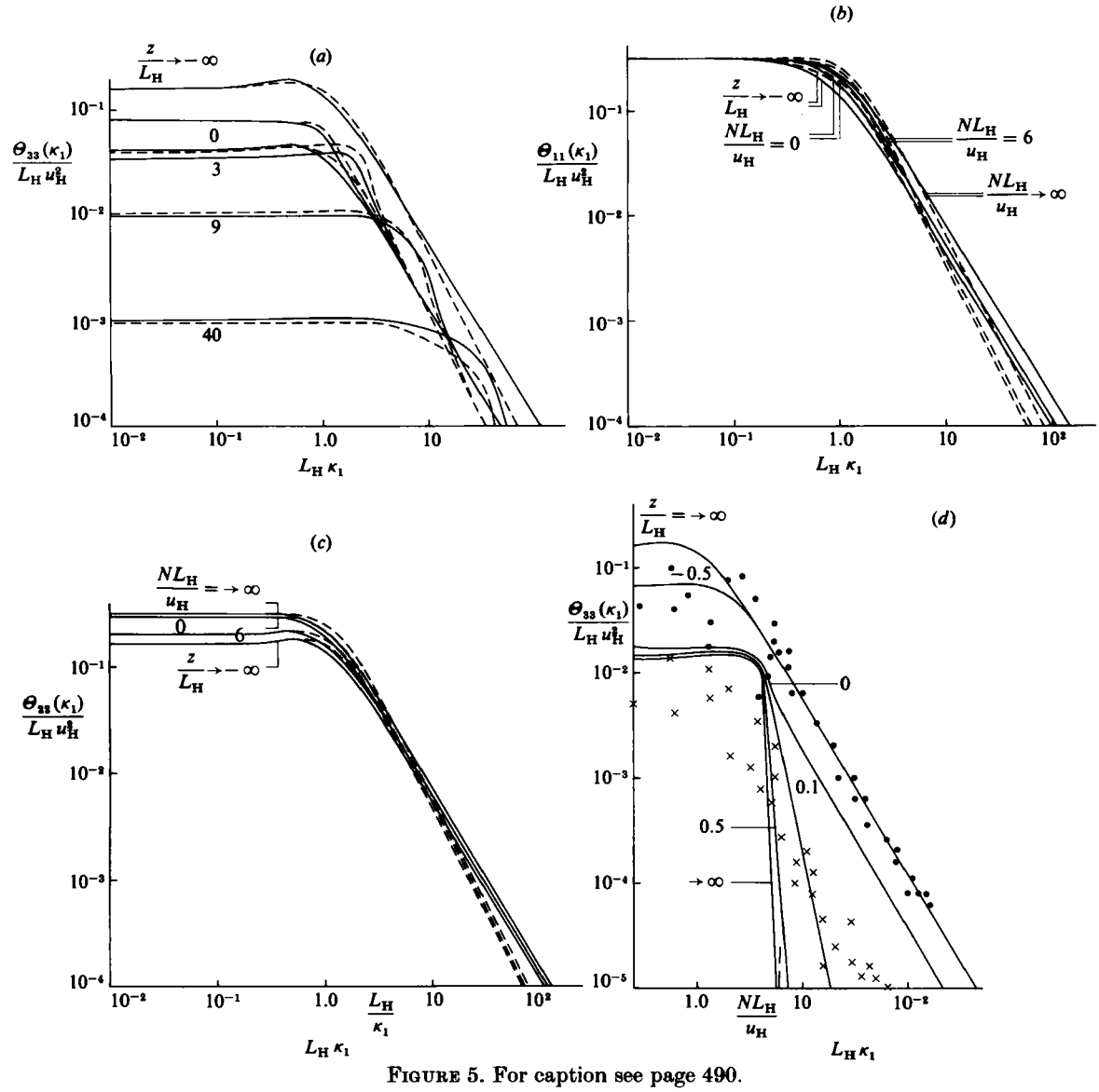

FIGURE 5. For caption see page 490.

minimum reactance to vertical motion by the stratified layer occurs when $k_{12} = N$ (in dimensional terms, $k_{12} u_H = N$). This reactance increases rapidly with decreasing k_{12} when $k_{12} < N$ because, the lower the wavenumber, the greater the disturbance would extend into the stratified region and the greater the energy required to make such a disturbance. The changes in $\Theta_{33}(\kappa_1)$ as a function of z show that there is a rapid fall-off, as z increases, in the high-frequency contribution for $\kappa_1 > N$; this is a result of the evanescent term decaying rapidly with height. At heights greater than about an integral scale above the interface ($z \geqslant L_H$), the spectra are almost entirely due to gravity waves, which in our inviscid model do not vary with z. (If, as is likely, absorption occurs at another level, that does not affect the solution near the interface.) These gravity-wave spectra have very sharp fall-offs in the high-frequency range. The measurements of Caughey & Palmer (1979) shown in the figures are discussed in detail in §3.2.

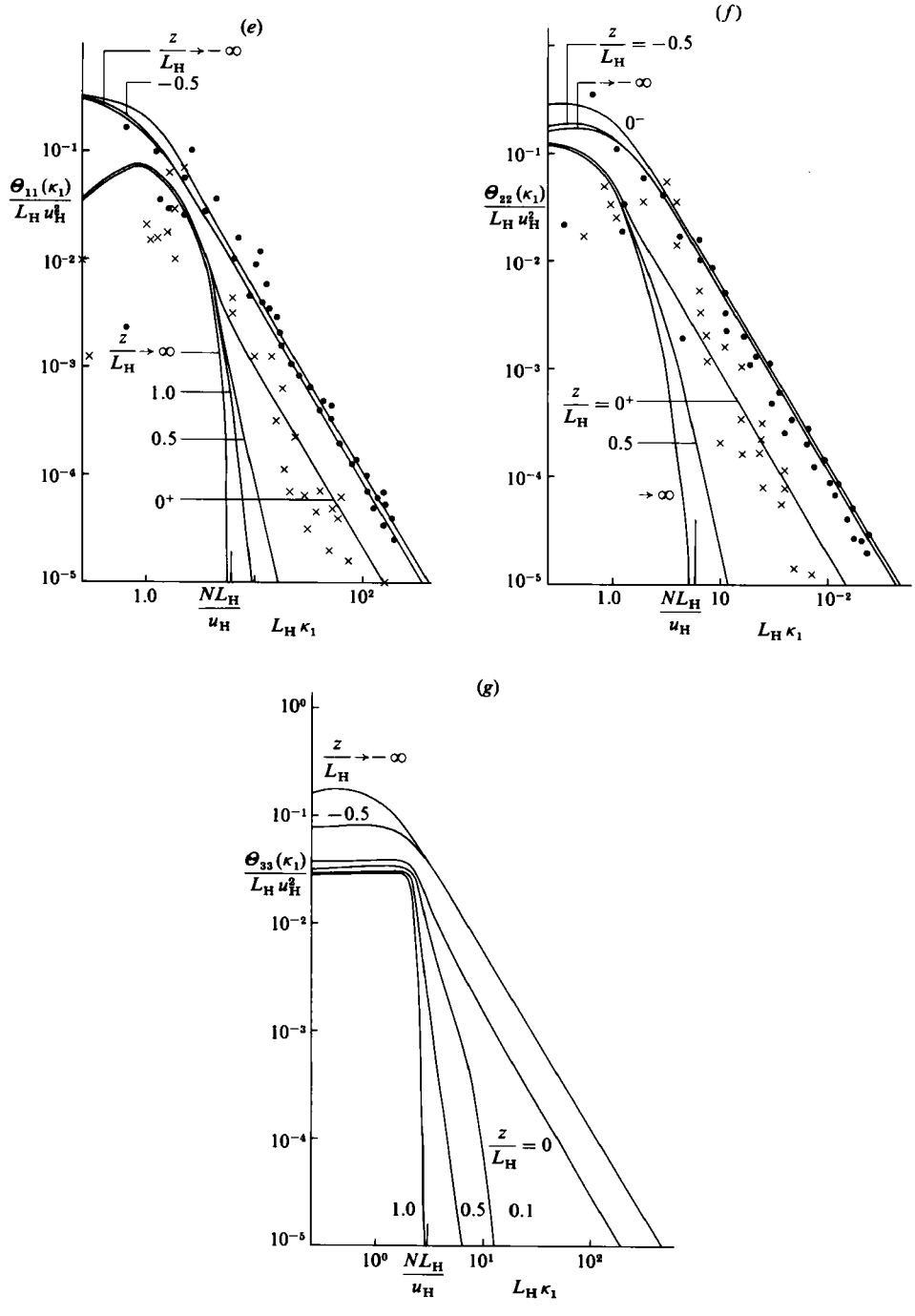

FIGURE 5. Calculated one-dimensional spectra for two forms of spectrum of homogeneous turbulence in the free stream compared with the experimental data of Caughey & Palmer (1979) where appropriate: ——, von Kármán spectrum; – – – – – –, Townsend spectrum. (*a*) Normal component at $z = 0$ for different values of NL_H/u_H. (*b*) Longitudinal component at $z = 0^-$. (*c*) Transverse component at $z = 0^-$. (*d*) Normal component for $NL_H/u_H = 6$. Measured: ●, $z = -0.1z_i$ ($\approx -0.2L_H$); ×, $z = -0.4z_i$ ($\approx 0.8L_H$). The interface is at $z = 0$ in our notation. (*e*) Longitudinal component. (*f*) Transverse component. (*g*) Normal component $NL_H/u_H = 3$.

2.5.2. *Variances*

Analytical expressions can be obtained for the gravity-wave contribution for $z \geqslant 0$ and for the evanescent contribution on $z = 0$.

Von Kármán form: $N \gg 1$

$$\overline{w_{\mathrm{g}}^2}(z \geqslant 0) = \tfrac{1}{12}\pi\gamma \frac{1}{N^{\frac{2}{3}}} \approx \frac{0.549}{N^{\frac{2}{3}}}, \tag{2.29a}$$

$$\overline{w_{\mathrm{e}}^2}(z = 0) = (\pi I(-\tfrac{1}{3})\tfrac{1}{9}\gamma)\frac{1}{N^{\frac{2}{3}}} \approx \frac{0.324}{N^{\frac{2}{3}}} \quad (\text{since } I(-\tfrac{1}{3}) \approx 0.442). \tag{2.29b}$$

Note that the results (2.29*a*, *b*) depend only on the form of the high-frequency part of the wavenumber-frequency spectrum which is universal and independent of its form at low wavenumbers. On $z = 0$ (2.29*a*) and (2.29*b*) reduce in dimensional terms to

$$\overline{w^2} = \overline{w_{\mathrm{g}}^2} + \overline{w_{\mathrm{e}}^2} \approx 0.873 u_{\mathrm{H}}^2 \left(\frac{u_{\mathrm{H}}}{NL_{\mathrm{H}}}\right)^{\frac{2}{3}}. \tag{2.29c}$$

The coefficient is determined by the definition of the von Kármán spectrum. Long (1978), in his theory of mixing in stably stratified fluid, finds that at $z = 0$

$$\overline{w^2} \propto u_{\mathrm{H}}^2 \left(\frac{u_{\mathrm{H}}}{NL_{\mathrm{H}}}\right). \tag{2.29d}$$

This result is given by our theory if a 'Lagrangian' rather than an 'Eulerian' frequency spectrum is used. If our expression for $\overline{w^2}$ in (2.29*c*) is used to estimate the entrainment rate by using Long's hypothesis, then the entrainment would be increased and be closer to observed values.

It is interesting that a similar expression to (2.29*c*) can be obtained on simple physical grounds. One assumes that, for large enough stratification, the turbulence is a function only of the 'Eulerian' frequency spectrum of the homogeneous turbulence at frequency N and of N itself, i.e.

$$\overline{w^2} = f(\phi^{\mathrm{H}}(\omega = N), N). \tag{2.30a}$$

Then, dimensional analysis of this expression leads to

$$\overline{w^2} = \frac{c u_{\mathrm{H}}^2}{(NL/u_{\mathrm{H}})^{\frac{2}{3}}}, \tag{2.30b}$$

where c is a constant and the expression is similar to (2.29*c*).

On $z = 0^+$,

$$\overline{u_{\mathrm{g}}^2}, \overline{v_{\mathrm{g}}^2} = \tfrac{1}{2} - \tfrac{1}{12}\pi\gamma \frac{1}{N^{\frac{2}{3}}} \approx \frac{1}{2} - \frac{0.549}{N^{\frac{2}{3}}}, \tag{2.31a}$$

$$\overline{u_{\mathrm{e}}^2}, \overline{v_{\mathrm{e}}^2} = \tfrac{1}{18}\pi\gamma\,(I(-\tfrac{1}{3}) - I(\tfrac{5}{3}))\frac{1}{N^{\frac{2}{3}}} \tag{2.31b}$$

$$\approx \frac{0.101}{N^{\frac{2}{3}}} \quad (\text{since } I(\tfrac{5}{3}) \approx 0.165).$$

Analytical expressions for the Townsend form of $\Phi_{ik}^{(\mathrm{H})}(\kappa)$ are shown in the Appendix.

The computed variances are shown in figure 6. Note that the vertical variance

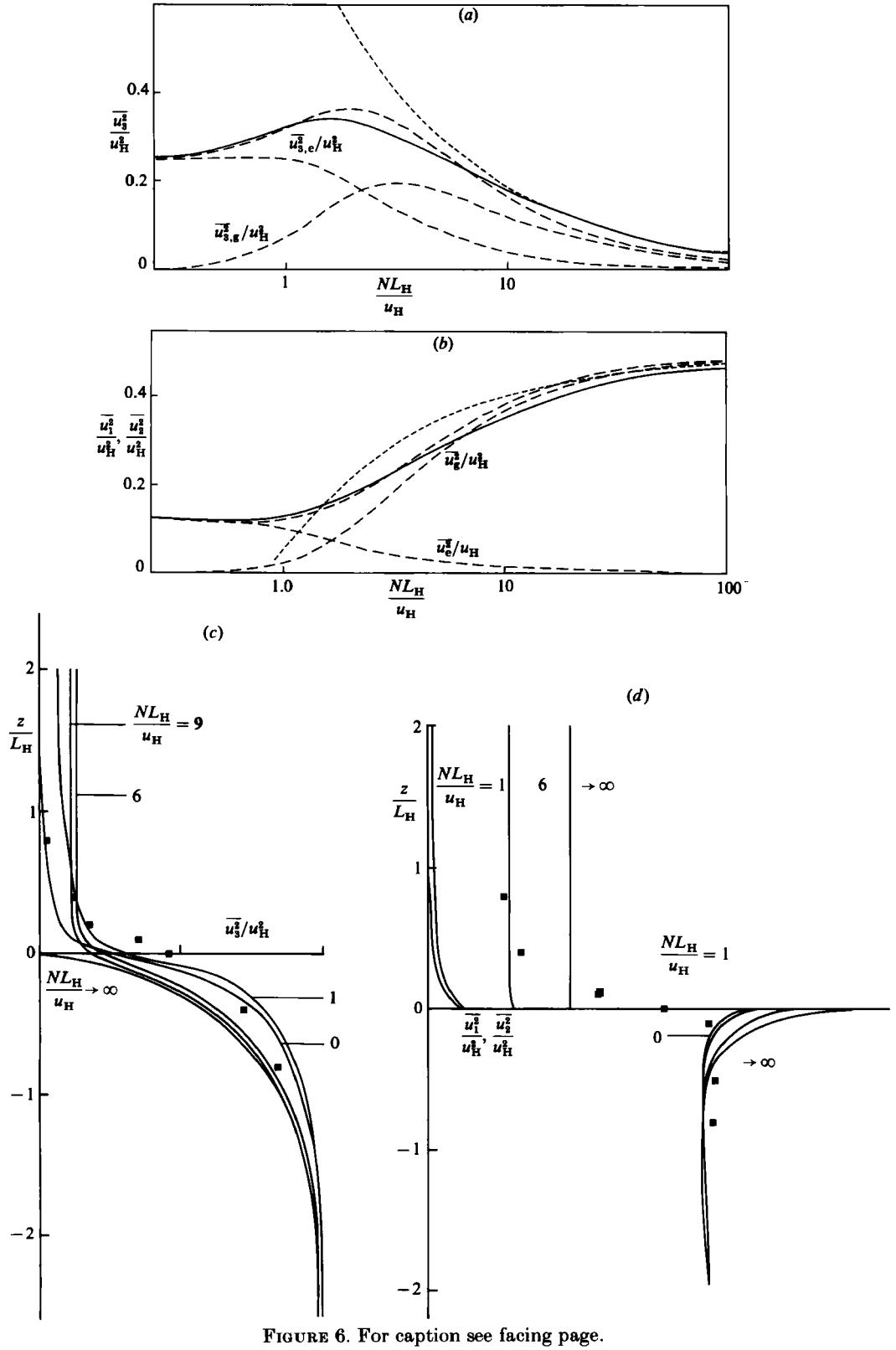

FIGURE 6. For caption see facing page.

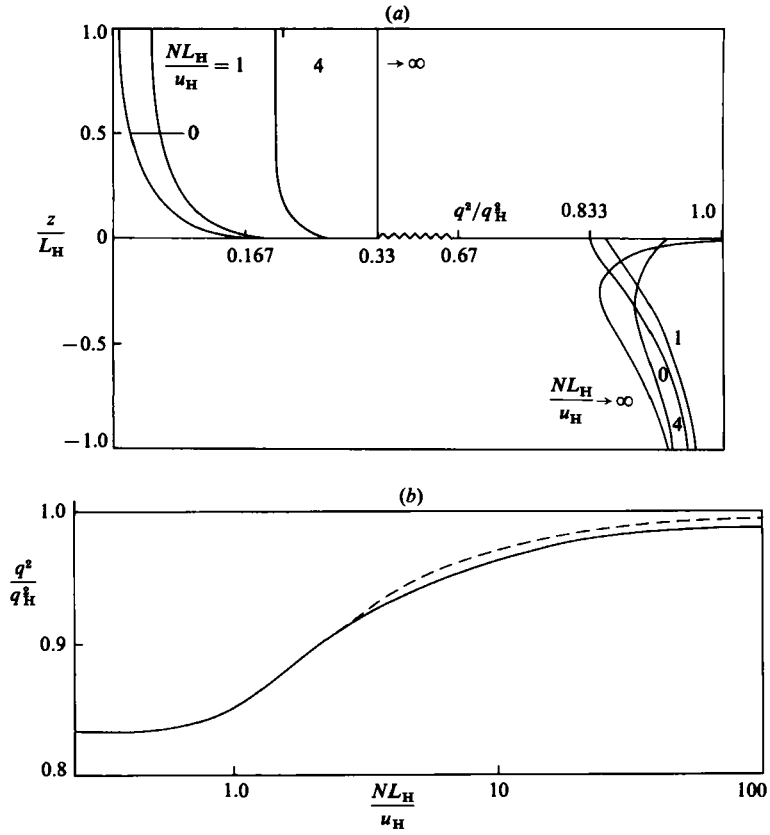

FIGURE 7. Turbulent kinetic energy q^2, (*a*) as a function of z for the von Kármán spectrum of free-stream turbulence, (*b*) at $z = 0^+$: ——, von Kármán spectrum; – – – – –, Townsend spectrum.

increases with N for small N with a maximum at $N \approx 2$ when $\overline{w^2}/u_H^2 \approx 0.35$ and the frequency of the energy-containing eddies corresponds approximately to N. The von Kármán spectrum results in greater vertical fluctuations for $N \gg 1$ since this spectrum has more energy in the smallest eddies. For the Townsend spectrum the contribution to the variances from frequencies $\omega > N$ and $\omega < N$ have been plotted separately in figures 6(*a*, *b*). For the case of vertical variances the evanescent contribution ($\omega > N$) decreases monotonically with NL_H/u_H whilst the gravity-wave contribution reaches a maximum at $NL_H/u_H \approx 5$. Measurements of Caughey & Palmer (1979) are plotted on the curves where appropriate. These are discussed in §3.2.

Plots of the total kinetic energy are shown in figure 7. Note that $q^2(z = 0^-) < q_H^2$ unless $N \to \infty$. Also, when in dimensional terms $NL_H/u_H \leqslant 3$, q^2 decreases monotonically with increasing z, whereas when $NL_H/u_H > 3$ there is a minimum in q^2 at $z/L_H \approx -0.2$.

FIGURE 6. Calculated variances for two forms of turbulence compared with the experimental observations of Caughey & Palmer (1979) where appropriate: ——, von Kármán spectrum; – – – – –, Townsend spectrum. (*a*) Normal component at $z = 0$: ....., asymptotic form for $NL_H/u_H \gg 1$, von Kármán spectrum. (*b*) Longitudinal and transverse components at $z = 0^+$. (*c*) Normal component as a function of z/L_H for different NL_H/u_H. Measured: ■, $NL_H/u_H = 6$. (*d*) Calculated longitudinal/transverse components. Measured component: ■, $NL_H/u_H = 6$.

2.5.3. *Integral scales*

These are defined as $L_x^{(u_i)} = (1/\overline{u^2})\int_{-\infty}^{\infty} \overline{u_i(x)\,u_i(x+r)}\,\mathrm{d}r$ and can be calculated analytically on $z = 0^-$ for $N \gg 1$, for the Von Kármán spectrum:

$$\frac{L_x^{(u)}}{L_H}(z=0, N \gg 1) = \frac{\Theta_{11}(\kappa_1 = 0, z = 0^-)}{\Theta_{11}^{(H)}(\kappa_1 = 0)} \frac{u_H^2}{\overline{u_1^2}(z=0)}, \tag{2.32a}$$

$$\approx \frac{2}{3}\left(1 + \frac{\delta}{N^{\frac{2}{3}}}\right) + O\left(\frac{1}{N^{\frac{5}{3}}}\right), \tag{2.32b}$$

where $\delta = \frac{1}{8}\gamma(1 - \frac{2}{3}(I(-\frac{1}{3}) - I(\frac{5}{3}))) \approx 0.298$, and $L_H = L_x^{(u)}$ for the homogeneous turbulence. Also for $N \gg 1$:

$$\frac{L_x^{(v)}}{L_H} = \frac{L_x^{(u)}}{L_H}; \quad \frac{L_x^{(w)}}{L_H} = \frac{3 + I(\frac{1}{3})}{(\frac{3}{4} + J(-\frac{1}{3}))}\frac{1}{N} \approx \frac{2.71}{N}. \tag{2.33}$$

In the limit $N \gg 1$ the theory predicts that at $z = 0$

$$\frac{L_x^{(w)}/L_H}{\overline{w^2}(z=0)/u_H^2} \propto \frac{1}{N^{\frac{1}{3}}}, \tag{2.34}$$

and the integral scale decreases at a faster rate with N than the vertical velocity variance.

The computed integral scales are plotted as functions of N and z in figure 8. Only the longitudinal scale of the vertical fluctuations $L_x^{(w)}$ is seen to vary significantly with stratification. Also plotted in figure 8(*c*) is the wavelength $\lambda_m^{(w)}$ at which $\kappa_1 \Theta_{33}(\kappa_1)$ is a maximum.

2.5.4. *Wave-energy flux in the stratified region*

The vertical energy flux in the stratified layer is given by

$$F_w = \overline{p'w'} = \iiint_{-\infty,\, k_{12} < N}^{\infty} \frac{k_{12}^2}{N^2}\left(\frac{N^2}{k_{12}^2} - 1\right)^{\frac{1}{2}} \Theta_{33}^{(H)}(\boldsymbol{\kappa})\,\mathrm{d}\kappa_1\,\mathrm{d}\kappa_2\,\mathrm{d}\kappa_3. \tag{2.35}$$

The flux is independent of z and for $N \gg 1$ is given by:

(in the von Kármán form)

$$F_w = \tfrac{1}{3}\pi\gamma\frac{1}{N^{\frac{2}{3}}} \approx \frac{2.20}{N^{\frac{2}{3}}}, \tag{2.36a}$$

(or in dimensional form)

$$\frac{F_w}{\bar{\rho}u_H^3} \approx 2.20\left(\frac{u_H}{NL_H}\right)^{\frac{2}{3}}, \tag{2.36b}$$

and for the Townsend spectrum

$$F_w = \frac{3}{2N}(\ln 2N - 1). \tag{2.37}$$

The computed fluxes and the asymptotic forms for $N \gg 1$ are shown in figure 9. An estimate of the importance to the convective boundary-layer development of the loss of energy due to gravity waves can be made by comparing the rate of energy (power P) lost by the turbulent fluid as wave energy to the energy-dissipation rate in the boundary-layer depth z_i

$$\frac{P_{\text{waves}}}{P_{\text{dissipation}}} = \frac{F_w \bar{\rho} u_H^3}{\epsilon \bar{\rho} z_i}, \tag{2.38}$$

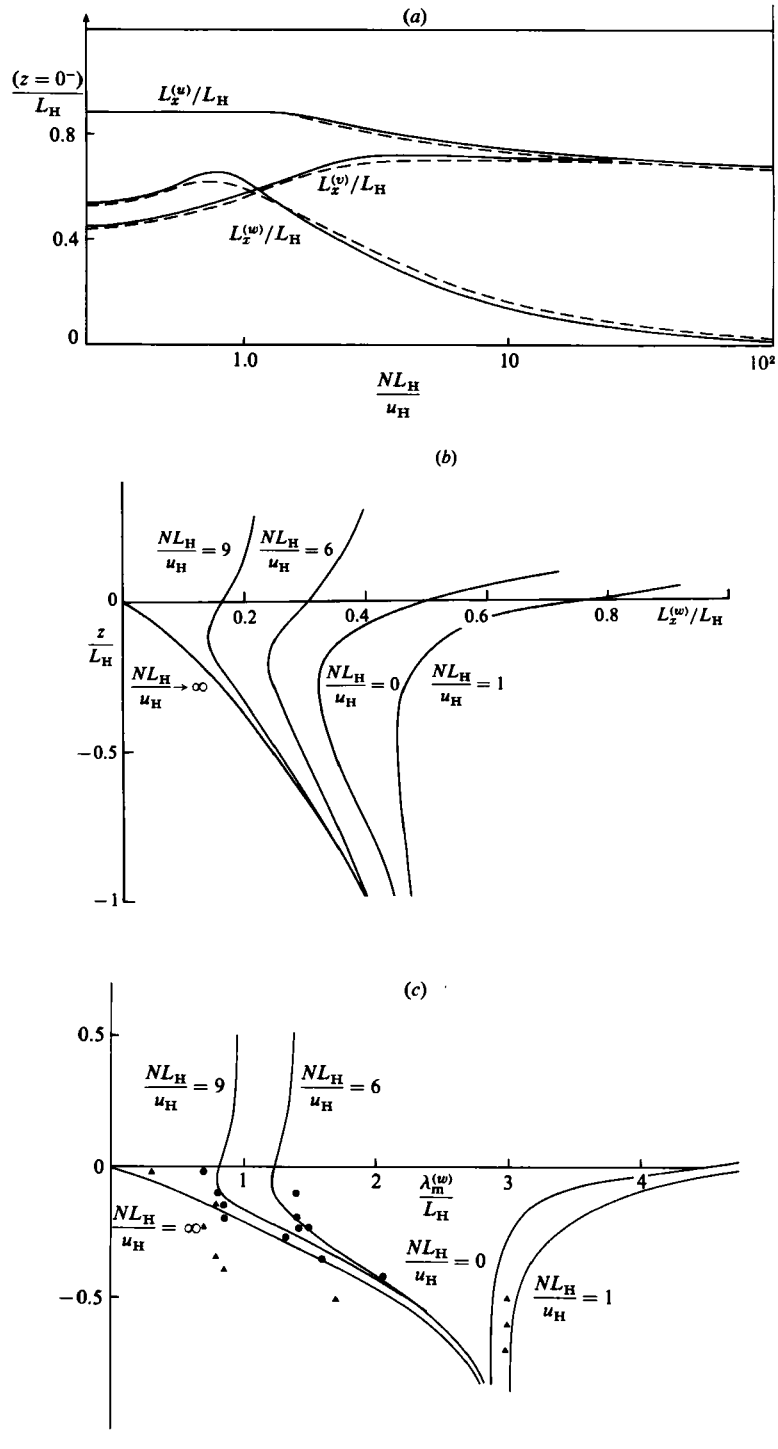

FIGURE 8. Integral scales and wavelengths. (*a*) Integral scales on $z = 0^-$ as a function of NL_H/u_H. (*b*) Vertical scales $L_x^{(w)}$ as a function of z. (*c*) The wavelength $\lambda_m^{(w)}$ at which $\kappa_1 \Theta_{33}(\kappa_1)$ is a maximum compared with the experimental data of Caughey & Palmer: $NL_H/u_H = 6$. The circles and triangles are from different data sets: ●, July 6; ▲, July 8.

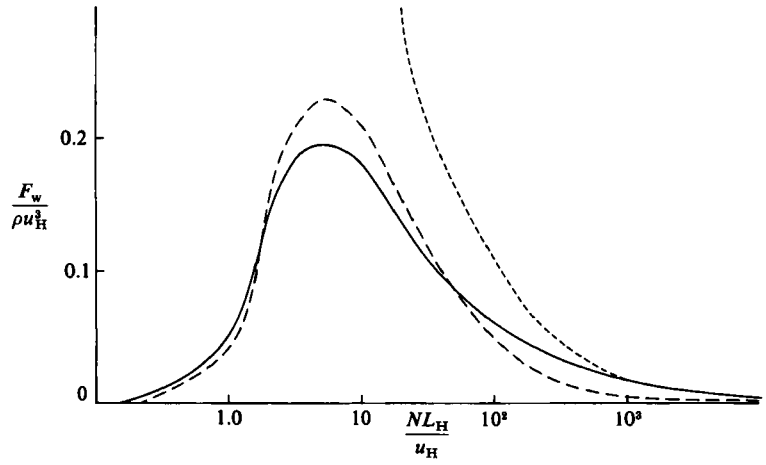

FIGURE 9. Calculated vertical wave flux in the stratified layer; ——, von Kármán spectrum; – – – – –, Townsend spectrum of free-stream turbulence. Asymptotic form for $NL_H/u_H \gg 1$; ....., von Kármán spectrum.

where ϵ is the energy-dissipation rate. Taking $z_1 = 2L_H$ and $\epsilon = u_H^3/L_H$ leads to

$$\frac{P_{\text{waves}}}{P_{\text{dissipation}}} = \tfrac{1}{2}F_w. \tag{2.39}$$

So, since the computations show $F_w \leqslant 0.2$, the loss of energy by waves is approximately an order of magnitude lower than the loss by dissipation throughout the depth of the boundary layer. However, the loss of energy by waves is of sufficient magnitude to have an important effect on the dynamics of the boundary layer because it is comparable with the energy dissipated near the inversion; hence there is less energy available for deepening the layer.

3. Discussion

3.1. *Limits of the model*

In the Introduction we suggested that the general class of turbulent flows confined by stratification can be subdivided into three main types: (i) the stable layer is uniformly stratified and there is no mean shear, (ii) there is an intensely stratified layer marking the edge of the turbulent layer with no shear, (iii) either of the first two cases with mean shear. The theory described in this paper is a model of type (i) only, so that comparisons with laboratory and field data are restricted to this situation.

The theory does not include the effect on the measured spectra and variances of the undulating motions at the interface caused by eddies impinging onto it. The effect of this on time-averaged measurements at a point is to blur the discontinuity in the structure of the horizontal components of turbulence across the interface. Gartshore, Durbin & Hunt (1983), in their use of rapid-distortion theory to describe the structure of motions in a shear layer outside a turbulent layer, estimated the effect by assuming that the position of the interface deviated from its mean position according to a Gaussian probability distribution.

Waves impinging on the interface from aloft are not considered by the theory. These have been described by Delisi & Orlanski (1975). They found that there was a

maximum in wave amplitude near the interface where incident and reflected waves interact. The amplitudes were small unless there was a thin region of stronger stratification marking the edge of the neutral layer; in this case wave breaking was observed to occur and large-amplitude waves were predicted by their theory.

3.2. *Comparison with experiment and numerical simulation*

There are few detailed observations and numerical simulations of structures of turbulence near an interface between a turbulent layer and a single uniformly stratified layer and the range of the non-dimensional buoyancy frequency is small; typically in the atmosphere $NL_{\mathrm{H}}/U_{\mathrm{H}} \approx 6$–$8$. Specific comparisons are made with the balloon measurements of Caughey & Palmer (1979) made in the dry atmospheric boundary layer, the laboratory experiment of Willis & Deardorff (1974) and the numerical simulations of Deardorff (1980), for his cases 1, 2 and 3. However, before discussing the comparisons we examine the extent to which the assumptions of the theory are satisfied in the experiments and numerical simulations.

3.2.1. *Conditions of the theory*

(1) *Energy dissipation rate.* The theory requires $\partial\epsilon/\partial z = 0$ or, more precisely,

$$\frac{1}{\epsilon}\frac{\partial \epsilon}{\partial z} \ll (L_x^{(w)})^{-1} \tag{3.1}$$

(Hunt 1984). This condition is well satisfied by the laboratory experiments of Willis & Deardorff and by the numerical simulations of Deardorff, where a balance of the turbulent-kinetic-energy equation requires $\partial\epsilon/\partial z \approx 0$. In Caughey & Palmer's measurements $(1/\epsilon)|\partial\epsilon/\partial z| \approx 1/2L_{\mathrm{H}}$.

(2) *Anisotropy.* The measurements of Caughey & Palmer show that the variances of the turbulent components in the centre of the boundary layer are approximately equal:

$$\overline{w^2} \approx \overline{u^2} \approx 0.4 w_*^2, \tag{3.2}$$

where $w_*^3 = g(\overline{w'\theta'}|_0/\bar{\theta})\, z_{\mathrm{i}}$, $\overline{w'\theta'}|_0$ is the surface heat flux, and z_{i} the depth of the boundary layer. This does not show that the turbulence is isotropic since boundary-layer convection usually consists of energetic upward motion of relatively small extent penetrating larger regions of slowly descending air (Lenschow & Stephens 1980), which is why the third-order moments $(\overline{w^3})$ are positive. However, the observed spectra do show the small-scale isotropy and universal spectral form assumed in the theory.

The computer simulations of Deardorff and laboratory experiments of Willis & Deardorff showed an anisotropic turbulent structure with

$$\frac{\overline{w^2}}{w_*^2} \approx 0.5, \quad \frac{\overline{u^2}}{w_*^2} \approx 0.2. \tag{3.3}$$

Thus for these cases comparisons with the theory can only be approximate.

(3) *Temperature/density gradient in the neutral layer.* The theory assumes that the turbulent region is sufficiently well mixed for the potential temperature to be uniform. However, entrainment of fluid from the stable layer is observed to cause low levels of stratification in the upper half of the turbulent region with, for the experiments and simulations referred to, buoyancy frequency $N \lesssim 4 \times 10^{-3}\ \mathrm{s}^{-1}$. This stratification may be expected to have a dynamic effect on scales L for which $u_{\mathrm{H}}/NL < 1$. This inequality is only satisfied for scales larger than the scale over which

Case	NL_H/u_H	$\overline{w^2}/w_0^2$ ($z = 0$) Observation/ simulation	$\overline{w^2}/w_0^2$ ($z = 0$) Theory	$\overline{w^2}/w_0^2$ ($z = 0.1L_H$) Observation/ simulation	$\overline{w^2}/w_0^2$ ($z = 0.1L_H$) Theory
Willis & Deardorff experiment					
1	7.0	0.26	0.21	0.39	0.16
2	10.0	0.18	0.16	0.09	0.11
Deardorff numerical simulation					
1	8.0	0.2	0.23		
2	7.1	0.3	0.24		
3	8.6	0.32	0.22		

TABLE 1. Vertical variances. Comparisons of the theory with the experiments of Willis & Deardorff and the numerical simulations of Deardorff.

the temperature gradient occurs, so dynamic effects are likely to be small and neglect of stratification in the turbulent layer is justified. The nonlinear effects caused by the interaction of eddies and fluctuating temperature gradients near the heated surface are discussed by Hunt (1984).

3.2.2. *Comparison*

(1) *Spectra.* The measured spectra of Caughey & Palmer are compared with the predictions of the theory in figures 6(*d–f*). The non-dimensional buoyancy frequency $NL_H/u_H = 6$, where we have taken $L_H = \frac{1}{2}z_i$, where z_i is the depth of the boundary layer ($z = 0$ at the boundary-layer top in our notation and the Earth's surface is at $z = -z_i$). For this case the atmospheric profile is given by Palmer, Caughey & Whyte (1979).

In his comparison of theory with atmospheric data, Hunt (1984) scales his results with the lengthscale $L_x^{(w)}$, the vertical integral scale in the centre of the convective boundary layer, and assumes $L_x^{(w)} = \frac{1}{4}z_i$ in agreement with atmospheric measurements. This assumption is consistent with our assumption ($L_H = \frac{1}{2}z_i$) since $L_H = L_x^{(u)}$ and in isotropic turbulence $L_x^{(u)} = 2L_x^{(w)} = 2L_x^{(v)}$.

The theoretical and experimental curves are in qualitative agreement, with the sharp fall-offs in the high-frequency ($\kappa_1 \gg N/u_H$) parts of the spectra for $z = z_i$; the residual high-frequency contribution in the measurements at $z = 0.4z_i$ is probably due to instrumental noise. The spectra of E. E. Gossard (private communication) calculated from Doppler radar measurements also show the same features in a stable layer well above the interface, although in that case the theory presented here is only appropriate in the deep stable layer some distance above the top of the mixed layer where there was a thin layer of intense stratification.

(2) *Variances.* The marked anisotropy of the boundary-layer turbulence in the experiments of Willis & Deardorff and in the numerical simulations of Deardorff makes precise comparison with the theory difficult; however, in all cases the observations are in agreement with the trends of the theory, with the vertical variances decreasing from their maximum values near the centre of the boundary layer as the interface is approached. The horizontal components show little variation over the entire mixed-layer depth, but there is some evidence of a small increase near the interface. Figures 6(*c*) and (*d*) show the measured values of Caughey & Palmer compared with the theory. The smooth profile in the time-averaged horizontal variance across the interface is caused by the undulating motions of the interface. Table 1 shows calculated and measured values of $\overline{w^2}/u_H^2$ at the interface. It is assumed

that $u_H = w_0$, where w_0 is the r.m.s. value of the observed vertical velocity at the centre of the mixed layer.

(3) *Lengthscales.* Figure 8(*c*) shows computed values of $\lambda_m^{(w)}$ (the wavelength at which $\kappa_1 \Theta_{33}(\kappa_1)$ is a maximum) and these are compared with the observations of Caughey & Palmer.

3.3. *Conclusions*

The linear theory developed in this paper describes the main features of the fluctuating velocities observed near an interface between a turbulent region and a stably stratified layer. A number of assumptions have been made in the theory that further experiments or numerical computation could test, viz. the relation between the Eulerian space-time spectra and the Eulerian space spectra, and the fact that the effect of the interface on the turbulent layer is to produce irrotational fluctuations. The most important physical parameter in the system is identified as the non-dimensional frequency NL_H/U_H; most results can be expressed in terms of this parameter. The important results of the theory are presented below.

(i) The vertical fluctuations decrease at the interface compared with their magnitude in the interior of the turbulent region for all NL_H/U_H, but are greatest at the interface for $NL_H/u_H \approx 2$ when $\overline{w}^2/u_H^2 \approx 0.35$. When $NL_H/ \gg 1$, $\overline{w}^2/u_H^2 \approx 0.87(u_H/NL_H)^{\frac{2}{3}}$. This is a slower rate of decrease with stratification than that suggested by Long (1978). When $NL_H/u_H \to 0$, $\overline{w}^2/u_H^2 \to 0.25$.

(ii) In the turbulent region at the interface the horizontal motion for large $NL_H/u_H \gg 1$ is given by $\overline{u}^2/u_H^2 \approx 1.5 - 0.4(u_H/NL_H^{\frac{2}{3}})$. ($\overline{v}^2 = \overline{u}^2$ throughout both layers.) When $NL_H/u_H \to 0$, $\overline{u}^2/u_H^2 \to 1.125$. There is a discontinuity in $\overline{u}^2$ independent of N given by $\Delta(\overline{u}^2) = u_H^2$. This discontinuity may lead to small-scale Kelvin–Helmholtz instabilities and entrainment by mechanism (1) described in the introduction.

(iii) In the stratified layer, waves with frequency $\omega > N$ decay rapidly with distance z from the interface and their contribution is negligible when $z/L_H > 1$. In this inviscid model, low-frequency waves ($\omega < N$) do not decay with height. Thus the high-frequency parts of the spectra fall off sharply, while in the low-frequency range there is no change with height.

(iv) At the interface the value of the longitudinal wavenumber at which the spectrum of vertical velocities reaches a maximum increases with increasing stratification. This occurs because eddies least affected by the stratified layer and hence those eddies which penetrate most easily into the stratified layer are those with a frequency $\omega \approx N$. It is likely that these eddies are important in the entrainment process, particularly in the third of the mechanisms described in the introduction.

(v) The vertical integral scale is smaller at the interface than in the interior of the turbulent region for all values of the stratification. At the interface it is a maximum when $NL_H \approx 1$, when $L_x^{(w)}/L_H \approx 0.65$, while for $NL_H/u_H \gg 1$, $L_x^{(w)}/L_H \approx 2.71$ (u_H/NL_H). The horizontal integral scales show little variation with stratification.

(vi) The wave energy flux (F_w) reaches a maximum of $F_w \approx 0.2\rho u_H^3$ when $NL_H/u_H \approx 6$; this value of the parameter is often observed in the atmosphere. When $NL_H/u_H \gg 1$ the flux decreases with increasing stratification and $F_w \approx 2.2$ (ρu_H^3) $(u_H/NL_H)^{\frac{2}{3}}$. The loss of energy by waves may have an important effect on the dynamics of the boundary layer.

During the work described here D.J.C. was supported by a fellowship provided by the Natural Environment Research Council.

Appendix. Analytic expressions

The one-dimensional spectra and variances can be calculated for $z \geqslant 0^+$, when $\omega > N$ and for $z = 0^+$ when $\kappa_1 = 0$ and $N \gg 1$. The integral scales can be calculated analytically in the turbulent region only on $z = 0^-$ when $N \gg 1$.

(i) One-dimensional spectra:

$$\Theta^{\mathrm{g}}_{33}(\kappa_1, z \geqslant 0^+) = \frac{3}{2\pi N^2}\left\{\frac{\kappa_1^4}{(1+\kappa_1^2)^2}(\alpha - \tfrac{1}{3}\alpha^3) + \frac{3\kappa_1^2 a^3}{(1+\kappa_1^2)} - \alpha - \tfrac{1}{3}\alpha^3 + \ln\left|\left(\frac{N^2-\kappa_1^2}{1+\kappa_1^2}\right)^{\frac{1}{2}} + \left(1+\frac{N^2-\kappa_1^2}{1+\kappa_1^2}\right)^{\frac{1}{2}}\right|\right\}, \tag{A 1}$$

where $\alpha^2 = (N^2-\kappa_1^2)/(N^2+1)$.

$$\Theta^{\mathrm{e}}_{33}(\kappa_1 = 0, z = 0^+, N \gg 1) = \frac{3}{2\pi N^2}(\ln 2 - \tfrac{1}{2}), \tag{A 2}$$

$$\Theta^{\mathrm{g}}_{11}(\kappa_1, z \geqslant 0^+) = \frac{3}{2\pi N^2}\left\{\frac{N^2-\kappa_1^2}{1+\kappa_1^2}\left(\alpha - \tfrac{1}{3}\alpha^3 - \frac{1}{3}\frac{1}{(1+\kappa_1^2)}\alpha^3\right)\right\}, \tag{A 3}$$

$$\Theta^{\mathrm{e}}_{11}(\kappa_1 = 0, z = 0^+) = 0, \tag{A 4}$$

$$\Theta^{\mathrm{g}}_{22}(\kappa_1, z \geqslant 0^+) = \frac{3}{2\pi N^2}\left\{\left(\frac{N^2-\kappa_1^2}{1+\kappa_1^2}\right)\tfrac{1}{3}\alpha^3 - \ln\left(\frac{N^2-\kappa_1^2}{1+\kappa_1^2}\right)^{\frac{1}{2}} + \left(1+\frac{N^2-\kappa_1^2}{1+\kappa_1^2}\right)^{\frac{1}{2}} + \alpha + \alpha^3\right\}, \tag{A 5}$$

$$\Theta^{\mathrm{e}}_{22}(\kappa_1 = 0, z = 0^+, N \gg 1) = \frac{3}{4\pi N^2}(\tfrac{3}{2}\ln 2 - \tfrac{7}{8}). \tag{A 6}$$

(ii) Variances:

$$\overline{w_{\mathrm{g}}^2} = \frac{3}{2N^2}\left\{\frac{\frac{8}{3}+N^2(4+N^2)}{(1+N^2)^{\frac{3}{2}}} - \frac{8}{3}\right\} \quad \text{for all } N,\ z \geqslant 0, \tag{A 7}$$

$$\overline{w_{\mathrm{e}}^2} = \frac{1}{2N}(N \gg 1, z = 0); \quad \overline{w_{\mathrm{e}}^2} + \overline{w_{\mathrm{g}}^2} = \frac{2}{N} \quad (N \gg 1, z = 0), \tag{A 8}$$

$$\overline{u_{\mathrm{g}}^2}, \overline{v_{\mathrm{g}}^2} = \frac{3}{4}\left\{\frac{2}{3} - \frac{\frac{2}{3}+N^2}{(N^2+1)^{\frac{3}{2}}} + \frac{1}{N^2}\left(\frac{8}{3} - \frac{\frac{8}{3}+4N^2+N^4}{(N^2+1)^{\frac{3}{2}}}\right)\right\} \quad \text{for all } N,\ z \geqslant 0^+, \tag{A 9}$$

$$\overline{u_{\mathrm{e}}^2}, \overline{v_{\mathrm{e}}^2}(N \gg 1, z = 0^+) = \frac{3}{16N}(\pi - 2) \approx \frac{0.214}{N}, \tag{A 10}$$

$$\overline{u^2}, \overline{v^2}(N \gg 1, z = 0^+) = \frac{1}{2} - \frac{1.714}{N}, \tag{A 11}$$

(iii) Integral scales:

$$L_x^{(u)}(N \gg 1,\ z = 0^+) = \frac{2}{3}\left(1+\frac{\sigma}{N}\right) + O\left(\frac{1}{N^2}\right), \tag{A 12}$$

where

$$\sigma = \tfrac{3}{4} - \tfrac{1}{8}\pi \approx 0.357), \tag{A 13}$$

$$\left.\begin{aligned} L_x^{(v)}(N \gg 1,\ z = 0^+) &= \frac{2}{3}\left(1+\frac{\sigma}{N}\right)\left(\frac{3}{2N^2}(\tfrac{1}{3}N^2 - \sinh^{-1}N + 2)\right) \\ &\approx \frac{2}{3}\left(1+\frac{\sigma}{N}\right) \end{aligned}\right\} \tag{A 14}$$

$$\left.\begin{aligned} L_x^{(w)}(N \gg 1,\ z = 0^+) &= \frac{3}{4N}(\ln N - 2\ln 2 - \tfrac{11}{6}) \\ &= \frac{3}{4N}(\ln N - 3.25). \end{aligned}\right\} \tag{A 15}$$

REFERENCES

BATCHELOR, G. K. 1953 *The Theory of Homogeneous Turbulence*. Cambridge University Press.

BROST, R. A., WYNGAARD, J. C. & LENSCHOW, A. H. 1982 Marine stratocumulus layers. Part II. Turbulence budgets. *J. Atmos. Sci.* **39**, 818–837.

CAUGHEY, S. J., CREASE, B. A. & ROACH, W. T. 1982 A field study of nocturnal stratocumulus. II. *Q. J. R. Met. Soc.* **198**, 125–144.

CAUGHEY, S. J. & PALMER, S. G. 1979 Some aspects of turbulence through the depth of the convective boundary layer. *Q. J. R. Met. Soc.* **105**, 811–827.

DEARDORFF, J. W. 1980 Stratocumulus-capped mixed layers derived from a three-dimensional model. *Boundary-Layer Met.* **18**, 495–527.

DELISI, D. P. & ORLANSKI, I. 1975 On the role of density jumps in the reflection and breaking of internal gravity waves. *J. Fluid Mech.* **69**, 445–464.

FERNANDO, H. J. S. & LONG, R. R. 1983 The growth of a grid-generated turbulent mixed layer in a two-fluid system. *J. Fluid Mech.* **133**, 377–396.

GARTSHORE, I. S., DURBIN, P. A. & HUNT, J. C. R. 1983 The production of turbulent stress in a shear flow by irrotational fluctuations. *J. Fluid Mech.* **137**, 307–330.

GOLDSTEIN, S. 1931 On the stability of a superimposed stream of fluids of different densities. *Proc. R. Soc. Lond.* A **132**, 524–548.

GOSSARD, E. E., CHADWICK, R. B., NEFF, W. D. & MORAN, K. P. 1982 The use of ground-based Doppler radars to measure gradients, fluxes and structure parameters in elevated layers. *J. Appl. Met.* **21**, 211–226.

HUNT, J. C. R. 1984 Turbulence structure in thermal convection and shear-free boundary layers. *J. Fluid Mech.* **138**, 161–184.

HUNT, J. C. R. & GRAHAM, J. M. R. 1978 Free-stream turbulence near plane boundaries. *J. Fluid Mech.* **84**, 209–235.

KAIMAL, J. C., WYNGAARD, J. C., AAUGEN, D. A., COTE, O. R., IZUMI, Y., CAUGHEY, S. J. & READINGS, C. J. 1976 Turbulence structure in the convective boundary layer. *J. Atmos. Sci.* **33**, 2151–2169.

KANTHA, L. H., PHILLIPS, O. M. & AZAD, R. S. 1978 On turbulent entrainment at a stable density interface. *J. Fluid Mech.* **79**, 753–768.

KATO, A. & PHILLIPS, O. M. 1969 On the penetration of a turbulent layer into a stratified liquid. *J. Fluid Mech.* **37**, 643–655.

LENSCHOW, D. H. & STEPHENS, P. L. 1980 *Boundary-Layer Met.* **19**, 509.

LINDEN, P. F. 1973 The interaction of a vortex ring with a sharp density interface: a model for turbulent entrainment. *J. Fluid Mech.* **60**, 467–480.

LONG, R. R. 1978 A theory of mixing in a stably stratified fluid. *J. Fluid Mech.* **84**, 113–124.

MCDOUGALL, T. J. 1979 Measurements of turbulence in a zero mean-shear mixed layer. *J. Fluid Mech.* **94**, 409–431.

PALMER, S. G., CAUGHEY, S. J. & WHYTE, K. W. 1979 An observational study of entraining convection using balloon-borne turbulence probes and high power Doppler radar. *Boundary-Layer Met.* **16**, 261–278.

PHILLIPS, O. M. 1955 The irrotational motion outside a free boundary layer. *Proc. Camb. Phil. Soc.* **51**, 220.

PIAT, J. F. & HOPFINGER, E. J. 1981 A boundary layer trapped by a density interface. *J. Fluid Mech.* **113**, 411–432.

PRICE, J. F. 1979 On the scaling of stress-driven entrainment experiments. *J. Fluid Mech.* **90**, 509–529.

STULL, R. B. 1976 Internal gravity waves generated by penetrative convection. *J. Atmos. Sci.* **33**, 1279–1286.

TENNEKES, H. 1975 Eulerian and Lagrangian time microscales in isotropic turbulence. *J. Fluid Mech.* **67**, 561–567.

TENNEKES, H. & LUMLEY, J. L. 1972 *A Short Course in Turbulence*, p. 293. MIT Press.

TOWNSEND, A. A. 1966 Internal waves produced by a convective layer. *J. Fluid Mech.* **24**, 307–319.

TURNER, J. S. 1973 *Buoyancy Effects in Fluids*, p. 368. Cambridge University Press.

WILLIS, G. E. & DEARDORFF, J. W. 1974 A laboratory model of the unstable planetary boundary layer. *J. Atmos. Sci.* **31**, 1297–1307.